Nonlinear Analysis: Modelling and Control, Online First, 1–26
https://doi.org/10.15388/namc.2026.31.46178

Vilnius University Press

Fixed-time distributed formation control for nonlinear heterogeneous multiagent systems subject to input nonlinearities and actuator faults

Jianmin Jiao[a,b], **Junmin Li**[a,1,2], **Chao He**[c], **Rui Zhang**[b]

[a] School of Mathematics and Statistics, Xidian University,
Shaanxi, Xi'an, 710126, China
jmjiao@126.com; jmli@mail.xidian.edu.cn

[b] School of Mathematics and Information Science,
Baoji University of Arts and Sciences,
Shaanxi, Baoji, 721013, China
zr0205@163.com

[c] School of Mathematics and Computer Science,
Shanxi Normal University,
Shanxi, Taiyuan, 030031, China
hechao@sxnu.edu.cn

Received: July 6, 2025 / **Revised:** December 20, 2025 / **Published online:** April 2, 2026

Abstract. This work focuses on distributed practical fixed-time formation (PFTF) control for heterogeneous multiagent systems (MASs) with inherent nonlinear dynamics, coupled input nonlinearities, and potential actuator faults. Conventional backstepping methods face the challenge of "differential explosion". To resolve this issue, we propose an innovative command filtering strategy with fixed-time convergence properties, integrated with a compensating mechanism that also ensures fixed-time suppression of filtering errors. Leveraging the synergy of fixed-time control theory, backstepping recursion, and neural networks function approximation, a distributed PFTF control protocol is developed. The designed scheme ensures that the MASs attain the predefined formation configuration within a fixed time, while driving all errors converge to a small residual set. Numerical simulations validate the effectiveness and performance of the proposed approach.

Keywords: multiagent systems (MASs), formation control, fixed time, input nonlinearity and actuator faults, command filtered backstepping.

1 Introduction

Distributed cooperative control of multiagent systems (MASs) has proven highly attractive due to its broad applicability in aerospace engineering, robotic manipulation, sensor networks, and smart grid systems. As extensively documented in [18], substantial progress

[1] The author was supported by the National Natural Science Foundation of China (62003254, 61573013).
[2] Corresponding author.

has occurred in this domain. The primary aim of cooperative control is realizing desired group behaviors through localized interactions among neighboring agents [34]. Formation control, as a crucial facet of MASs coordination, requires that all agents maintain predetermined configurations for effective task execution [5]. Heterogeneous MASs, featuring agents with distinct dynamics, have garnered growing research interest owing to their enhanced practical relevance over homogeneous counterparts. Notable strides have been made in tackling formation control for heterogeneous MASs. For instance, [30] established an adaptive formation protocol for linear MASs exhibiting heterogeneous uncertainties. Cao et al. [2] combined backstepping techniques with fuzzy-logic approaches to devise a formation strategy for nonlinear MASs possessing unmeasurable states. [28] leveraged command filter technology to circumvent the "differential explosion" problem in nonlinear MASs, introducing a collision-free intelligent formation control methodology. However, practical engineering deployments impose rigorous demands on convergence speed – a vital performance metric conspicuously unaddressed in these studies [2, 28, 30]. The aforementioned schemes ensure solely asymptotic convergence, implying theoretically infinite settling time for formation attainment, which presents a fundamental limitation for time-constrained missions.

Significant progress in finite-time control has markedly enhanced convergence rates for MASs, particularly for heterogeneous MASs in consensus [3, 6], formation [26, 27], and containment [13] control. Building on these advances, fixed-time control strategies were introduced in [15], establishing the theoretical foundation for convergence with a uniform upper-bound settling time independent of initial conditions [12]. This breakthrough has triggered widespread investigation into fixed-time control [10, 14, 20], positioning it as a key research frontier for MASs, with substantial developments in consensus [9, 29, 35] and formation control [1, 7, 11, 23, 25]. For instance, studies [11] and [23] respectively tackled practical fixed-time formation (PFTF) control for disturbed second-order linear and nonlinear MASs. The authors in [1] presented a fixed-time prescribed performance formation control method for nonlinear high-order MASs. Utilizing nonlinear transformation functions, the works in [7] and [25] addressed the full-state constrained PFTF and optimized PFTF control problems for nonlinear MASs, respectively. However, existing approaches reveal notable limitations: the protocols in [11] and [23] are applicable only to second-order systems; the strategy in [1] guarantees solely fixed-time convergence of formation errors; and the interaction topologies considered in [7] and [25] assume undirected communication. Moreover, critical challenges remain when handling strongly heterogeneous MASs featuring diverse nonlinear dynamics, varying control gains, distinct disturbances, mixed-order systems, and coupled input nonlinearities with actuator faults. Collectively, these limitations highlight the urgent need for unified fixed-time formation control frameworks capable of managing such complex heterogeneous MASs, motivating this research.

Input nonlinearities combined with actuator faults significantly threaten system stability and operational reliability. Typical input nonlinearities, such as saturation, dead-zone, hysteresis, and quantization effects, were unified in [24] for nonlinear system tracking control. Actuator faults are equally critical, and their impacts are amplified in MASs due to two factors: first, the inherent scalability of MASs elevates fault probability as

the number of agents increases; second, performance degradation induced by faults can propagate across interaction networks, potentially compromising overall system functionality [17]. While existing cooperative control schemes have successfully handled isolated input nonlinearities or actuator faults, the complex interdependencies arising from their simultaneous occurrence, particularly nonaffine actuator faults [3], remain insufficiently explored in current research. This critical knowledge gap further motivates the present study.

Building on the above discussion, this paper focuses on the PFTF control problem for heterogeneous MASs subject to both input nonlinearities and actuator faults. The study advances PFTF control methodology through three key contributions:

(i) A novel distributed PFTF control framework for heterogeneous MASs is established, significantly extending the existing research architecture on MASs formation control. This scheme incorporates heterogeneity–encompassing diverse nonlinear dynamics, variable control gains, external disturbances, and arbitrary system orders, thereby addressing key limitations of prior work.

(ii) Distinct from asymptotic and finite-time formation methods, the proposed strategy ensures fixed-time formation achievement for MASs. Compared to existing fixed-time approaches, the scheme employs a less conservative stability criterion derived from [10]. A pivotal advancement is the introduction of a key inequality via Lemma 8 to enable fixed-time formation performance analysis. This lemma generalizes stability analysis tools prevalent in adaptive finite-time and fixed-time control frameworks, such as those in [4, 14, 20, 35].

(iii) An enhanced fixed-time command filter architecture coupled with a novel error compensation mechanism is developed. The proposed filter offers dual advantages over existing designs: compared to filters in [1, 6, 10, 19, 21, 28], it resolves the "differential explosion" problem while improving parameter tunability; unlike the design in [8], it eliminates piecewise functions, thereby simplifying convergence analysis.

The remaining structure of this paper is arranged as follows: Section 2 focuses on the formulation of the research problem and the collation of prerequisite knowledge. Section 3 is dedicated to the design of control protocols and the analytical study on fixed-time formation performance. Section 4 carries out simulation verification and presents detailed analysis of the simulation results. Section 5 outlines the main conclusions and summaries of the paper.

2 Problem formulation and preliminaries

2.1 Problem formulation

Consider a MASs comprising one leader and M followers. Interactions among followers are modeled by a directed graph $\mathcal{G} = (\mathcal{V}, \mathcal{E}, \mathcal{A})$. Here $\mathcal{V} = \{1, 2, \ldots, M\}$ is the node set, $\mathcal{E} = \{(i, j),\, i, j \in \mathcal{V},\, i \neq j\}$ is the edge set with $(i, j) \in \mathcal{E}$ indicating that agent i receives information from agent j. $\mathcal{A} = [a_{ij}] \in \mathbb{R}^{M\times M}$ is the adjacency

matrix, where $a_{ij} = 1$ if $(i,j) \in \mathcal{E}$, and $a_{ij} = 0$ otherwise. The degree matrix is defined as $\mathcal{H} = \operatorname{diag}\{h_1, h_2, \ldots, h_M\}$ with $h_i = \sum_{j=1,\, j\neq i}^{M} a_{ij}$. The Laplacian matrix is $\mathcal{L} = \mathcal{H} - \mathcal{A}$. Communication between followers and the leader is described by $\mathcal{B} = \operatorname{diag}\{b_1, b_2, \ldots, b_M\}$, where $b_i = 1$ if follower i receives information directly from the leader, and $b_i = 0$ otherwise.

Assumption 1. (See [19].) For each follower, at least one directed path exists from the leader to that follower.

The dynamics of the ith follower ($i = 1, 2, \ldots, M$) are governed by the following high-order nonlinear system:

$$\begin{aligned}
\dot{x}_{i,j} &= g_{i,j}(\bar{x}_{i,j})x_{i,j+1} + f_{i,j}(\bar{x}_{i,j}) + \omega_{i,j}(t) \quad (j = 1, 2, \ldots, \Upsilon_i - 1),\\
\dot{x}_{i,\Upsilon_i} &= g_{i,\Upsilon_i}(\bar{x}_{i,\Upsilon_i})\bar{u}_i + f_{i,\Upsilon_i}(\bar{x}_{i,\Upsilon_i}) + \omega_{i,\Upsilon_i}(t),\\
\bar{u}_i &= u_i\big(v_i(t)\big) + J_i(t-\tau_i)\Pi_i(\bar{x}_{i,\Upsilon_i}, u_i),\\
y_i &= x_{i,1},
\end{aligned} \tag{1}$$

where $\bar{x}_{i,j} = [x_{i,1}, x_{i,2}, \ldots, x_{i,j}]^{\mathrm{T}} \in \mathbb{R}^j$ is the state vector. $\bar{u}_i \in \mathbb{R}$ and $v_i \in \mathbb{R}$ denote actuator and controller outputs, respectively. $y_i \in \mathbb{R}$ is the system output. $\omega_{i,j}(t) \in \mathbb{R}$ represents bounded external disturbances. $g_{i,j}(\bar{x}_{i,j})$ and $f_{i,j}(\bar{x}_{i,j})$ are known and unknown smooth nonlinear functions, respectively. The input nonlinearity $u_i(v_i(t)) \in \mathbb{R}$ is modeled as

$$u_i\big(v_i(t)\big) = h_i(t)v_i(t) + \sigma_i(t), \tag{2}$$

where $h_i(t)$ is an unknown continuous function with $|h_i(t)| \in L_i = [\underline{h}_i, \bar{h}_i]$ for unknown constants $\bar{h}_i > \underline{h}_i > 0$. $\sigma_i(t)$ is an unknown bounded function satisfying $|\sigma_i(t)| \leqslant \bar{\sigma}_i$ for unknown constant $\bar{\sigma}_i > 0$. The term $J_i(t-\tau_i)\Pi_i(\bar{x}_{i,\Upsilon_i}, u_i)$ models a nonaffine actuator fault, where $\Pi_i(\bar{x}_{i,\Upsilon_i}, u_i)$ is a nonlinear fault function, $J_i(t-\tau_i)$ is the fault activation function

$$J_i(t-\tau_i) = \begin{cases} 0, & t < \tau_i,\\ 1 - \mathrm{e}^{-\zeta_i(t-\tau_i)}, & t \geqslant \tau_i, \end{cases} \tag{3}$$

with constant $\zeta_i > 0$. Small ζ_i values characterize incipient faults, while large values indicate abrupt faults.

Assumption 2. (See [24, 31].) The known smooth nonlinear functions $g_{i,j}(\bar{x}_{i,j})$ satisfy $0 < \underline{g}_{i,j} \leqslant |g_{i,j}(\bar{x}_{i,j})| \leqslant \bar{g}_{i,j}$, where $\underline{g}_{i,j}$ and $\bar{g}_{i,j}$ denote unknown positive constants.

Assumption 3. (See [24,31].) External disturbances $\omega_{i,j}(t)$ are bounded, i.e., $|\omega_{i,j}(t)| \leqslant \bar{\omega}_{i,j}$ for unknown positive constants $\bar{\omega}_{i,j}$.

Assumption 4. (See [3, 17].) Actuator faults satisfy the inequality

$$\big|g_{i,\Upsilon_i}(\bar{x}_{i,\Upsilon_i})J_i(t-\tau_i)\Pi_i(\bar{x}_{i,\Upsilon_i}, u_i) + f_{i,\Upsilon_i}(\bar{x}_{i,\Upsilon_i})\big| \leqslant \bar{f}_{i,\Upsilon_i}(\bar{x}_{i,\Upsilon_i}, u_i),$$

where $\bar{f}_{i,\Upsilon_i}(\bar{x}_{i,\Upsilon_i}, u_i)$ is an unknown continuous function.

Remark 1. Agents in (1) exhibit strong heterogeneity manifested through: distinct nonlinear functions $f_{i,j}(\bar{x}_{i,j})$, different control gains $g_{i,j}(\bar{x}_{i,j})$, varying disturbances $\omega_{i,j}(t)$, nonidentical input nonlinearities $u_i(v_i(t))$, diverse actuator faults $J_i(t-\tau_i)\Pi_i(\bar{x}_{i,\Upsilon_i}, u_i)$, heterogeneous system orders Υ_i. This multifaceted heterogeneity prevents direct application of existing control protocols [1, 7, 11, 23, 25] to the PFTF problem for MASs (1).

Remark 2. Control inputs in practical applications frequently encounter multiple nonlinear constraints, including dead-zone, saturation, and hysteresis – all effectively characterized by model (2) [24]. Compounding these issues, real-world systems often experience time-varying nonaffine actuator faults described by (3) [17]. These factors highlight the importance of investigating PFTF control within a unified framework addressing both input nonlinearities and actuator faults simultaneously.

The leader's reference output is denoted by $y_r(t) \in \mathbb{R}$. The desired formation configuration is specified by $\xi(t) = [\xi_1(t), \xi_2(t), \ldots, \xi_M(t)]^{\mathrm{T}} \in \mathbb{R}^M$. This study designs adaptive distributed controllers $v_i(t)$ for each follower to achieve:

(i) PFTF: $|y_i(t) - y_r(t) - \xi_i(t)| \leqslant \delta$ for all $t \geqslant T$, $i = 1, 2, \ldots, M$, for some fixed time $T > 0$ and adjustable constant $\delta > 0$ (PFTF error bound).

(ii) Boundedness of all closed-loop signals and convergence of all errors (including filter and parameter estimation errors) to a residual set near the origin within fixed time T.

Assumption 5. (See [19, 27].) The reference signal $y_r(t)$ and formation functions $\xi_i(t)$ are twice continuously differentiable with bounded first and second derivatives.

Remark 3. Assumption 1 ensures that each follower can acquire the leader's information either directly or indirectly. As indicated in [19], this serves as a prerequisite for the distributed realizability of the control objectives. Assumption 2 implies that the functions $g_{i,j}(\bar{x}_{i,j})$ are bounded and are each either entirely positive or entirely negative, which is necessary to ensure the controllability of the system. Assumption 3 embodies the bounded characteristic of disturbances, a feature ubiquitous in practical applications. Both Assumptions 2 and 3 are standard and consistent with the works of [24, 31]. Assumption 4 provides nonaffine fault tolerance conditions following [3, 17], which can be interpreted as integrating faults into a continuous nonlinear function $\bar{f}_{i,\Upsilon_i}(\bar{x}_{i,\Upsilon_i}, u_i)$. It should be noted that the function $\bar{f}_{i,\Upsilon_i}(\bar{x}_{i,\Upsilon_i}, u_i)$ is independent of the fault occurrence time τ_i, thus eliminating the dependence of the obtained results on τ_i; in other words, the resulting control scheme is applicable to any unknown τ_i. Assumption 5 guarantees operational smoothness in practical implementations. Similar assumptions commonly adopted in the literature, as seen in [19, 27].

2.2 Preliminaries

Lemma 1. (*See* [10].) *Consider the system* $\dot{\Gamma} = \psi(\Gamma)$ *with* $\psi(0) = 0$. *If there exists a Lyapunov function* $W(\Gamma)$ *satisfying*

$$\dot{W}(\Gamma) \leqslant -\gamma_1 W(\Gamma) - \gamma_2 W^{\Delta_1}(\Gamma) - \gamma_3 W^{\Delta_2}(\Gamma) + \gamma_0,$$

where $\gamma_0, \gamma_1, \gamma_2, \gamma_3 > 0$, $0 < \Delta_1 < 1$, and $\Delta_2 > 1$, then the origin is practical fixed-time stable (PFTS). The settling time $T(\Gamma_0)$ is bounded by

$$\begin{aligned} T(\Gamma_0) &\leqslant T \\ &= \max\left\{\frac{\ln(1+\frac{\gamma_1}{\iota\gamma_2})}{\gamma_1(1-\Delta_1)}, \frac{\ln(1+\frac{\iota\gamma_1}{\gamma_2})}{\iota\gamma_1(1-\Delta_1)}\right\} + \max\left\{\frac{\ln(1+\frac{\gamma_1}{\iota\gamma_3})}{\gamma_1(\Delta_2-1)}, \frac{\ln(1+\frac{\iota\gamma_1}{\gamma_3})}{\iota\gamma_1(\Delta_2-1)}\right\}, \end{aligned}$$

and for $t \geqslant T$,

$$\Gamma \in \left\{\Gamma \;\middle|\; W(\Gamma) \leqslant \min\left\{\frac{\gamma_0}{(1-\iota)\gamma_1}, \left(\frac{\gamma_0}{(1-\iota)\gamma_2}\right)^{1/\Delta_1}, \left(\frac{\gamma_0}{(1-\iota)\gamma_3}\right)^{1/\Delta_2}\right\}\right\}$$

with $0 < \iota < 1$.

Lemma 2. (*See* [16].) *For $\varrho > 0$ and $\zeta \in \mathbb{R}$, there is*

$$0 \leqslant |\zeta| - \zeta \tanh\frac{\zeta}{\varrho} \leqslant \iota_0 \varrho,$$

where $\iota_0 = 0.2785$.

Lemma 3. (*See* [35].) *For $\varrho > 0$ and $\zeta_l \in \mathbb{R}$ ($l = 1, 2, \ldots, M$), there is*

$$\left(|\zeta_1| + \cdots + |\zeta_M|\right)^{\varrho} \leqslant \max\left\{M^{\varrho-1}, 1\right\}\left(|\zeta_1|^{\varrho} + \cdots + |\zeta_M|^{\varrho}\right).$$

Lemma 4. (*See* [16].) *For continuous functions $F(\Theta)$ defined on compact set Ω and any approximation accuracy $\bar{\varepsilon} > 0$, there exists a neural networks (NNs) approximation*

$$F(\Theta) = \theta^{\mathrm{T}}\varphi(\Theta) + \varepsilon(\Theta)$$

with ideal weight vector $\theta = [\theta_1, \theta_2, \ldots, \theta_m]^{\mathrm{T}} \in \mathbb{R}^m$, bounded approximation error $|\varepsilon(\Theta)| \leqslant \bar{\varepsilon}$, and Gaussian basis functions $\varphi(\Theta) = [\varphi_1(\Theta), \varphi_2(\Theta), \ldots, \varphi_m(\Theta)]^{\mathrm{T}}$. Here ς_i and l_i denote the center and width of the Gaussian function, respectively.

Lemma 5. (*See* [6].) *Given basis function vector $\varphi(\Theta) = [\varphi_1(\Theta), \varphi_2(\Theta), \ldots, \varphi_m(\Theta)]^{\mathrm{T}}$, define $\Theta_1 = [x_1, x_2, \ldots, x_{m_1}]^{\mathrm{T}}$ and $\Theta_2 = [x_1, x_2, \ldots, x_{m_2}]^{\mathrm{T}}$ with $m_1 \geqslant m_2$. Then it holds*

$$\varphi^{\mathrm{T}}(\Theta_1)\varphi(\Theta_1) \leqslant \varphi^{\mathrm{T}}(\Theta_2)\varphi(\Theta_2).$$

Lemma 6. (*See* [29].) *For $\varrho > 0$, $\zeta_1 \geqslant 0$, $\zeta_2 > 0$, and $\zeta_1 \geqslant \zeta_3$, the following inequalities hold*:

$$\zeta_1^{\varrho}(\zeta_2 - \zeta_1) \leqslant \frac{1}{1+\varrho}\left(\zeta_2^{1+\varrho} - \zeta_1^{1+\varrho}\right)$$

and

$$\zeta_3^{\varrho+1} - \zeta_1^{\varrho+1} \leqslant (\zeta_1 - \zeta_3)^{\varrho+1}.$$

Lemma 7. (*See* [31].) *Let* $V(t) \geqslant 0$ *and* $\vartheta_i(t)$ $(i = 1, 2, \ldots, M)$ *be smooth functions on* $[0, \infty)$. *If*

$$\dot{V}(t) \leqslant -CV(t) + \sum_{i=1}^{M} \big[h_i(t)N\big(\vartheta_i(t)\big) + p\big]\dot{\vartheta}_i(t) + q,$$

where p, q, *and* $C > 0$ *are constants,* $N(\vartheta_i)$ *is a Nussbaum function, and* $h_i(t)$ *are continuous functions satisfying* $|h_i(t)| \in L_i = [\underline{h}_i, \bar{h}_i]$ *with* $\bar{h}_i > \underline{h}_i > 0$, *then both* $V(t)$ *and* $\vartheta_i(t)$ *remain bounded for all* $t \in [0, \infty)$.

Lemma 8. *Consider the dynamical system*

$$\dot{\Phi}(t) = \Psi_1\big(\Phi(t)\big) + \Psi_2(t),$$

where $\Phi(t)$, $\Psi_1(\Phi)$, *and nonnegative* $\Psi_2(t)$ *are continuously differentiable functions. If* $\Psi_1(\Phi) \geqslant 0$ *for* $\Phi \leqslant 0$ *and initial condition* $\Phi(t_0) \geqslant 0$, *then* $\Phi(t) \geqslant 0$ *holds for all* $t \geqslant t_0$.

Proof. Suppose there exists a time $t_1 > t_0$ such that $\Phi(t_1) < 0$. Define the zero-crossing set

$$\aleph = \big\{t \;\big|\; \Phi(t) = 0,\ t \in [t_0, t_1]\big\}.$$

Continuity of $\Phi(t)$ and initial condition $\Phi(t_0) \geqslant 0$ imply $\aleph \neq \emptyset$. Let $t_2 = \sup\aleph \in [t_0, t_1]$. To show $t_2 \in \aleph$, assume otherwise. By supremum properties, for $m = 1, 2, \ldots$, there exist $t_m^* \in \aleph \cap (t_2 - (t_2 - t_o)/m,\ t_2)$. Thus, we obtain

$$0 = \lim_{m\to\infty} \Phi(t_m^*) = \lim_{t\to t_2^-} \Phi(t) = \Phi(t_2),$$

contradicting $t_2 \notin \aleph$. Hence $t_2 \in \aleph$. For $t \in [t_2, t_1]$, we have $\Phi(t) \leqslant 0$. The nonnegativity assumptions give $\dot{\Phi}(t) \geqslant 0$, implying that $\Phi(t)$ is nondecreasing on $[t_2, t_1]$. Thus, $\Phi(t_2) \leqslant \Phi(t_1)$, but $\Phi(t_1) < 0$ and $\Phi(t_2) = 0$ create contradiction. Therefore, $\Phi(t) \geqslant 0$ holds for all $t \geqslant t_0$. □

Remark 4. Lemma 8 will be implemented by selecting

$$\Psi_1\big(\Phi(t)\big) = -\Gamma_1\Phi(t) - \Gamma_2\Phi^{\alpha}(t) - \Gamma_3\Phi^{\beta}(t), \qquad \Phi(t_0) \geqslant 0,$$

where $\Gamma_1, \Gamma_2, \Gamma_3 > 0$, $0 < \alpha < 1$, $\beta > 1$, and α, β are ratios of odd integers (the definitions of α and β remain consistent throughout the subsequent text). This formulation generalizes recent results [4, 14, 20, 35], which correspond to special cases, and provides broader applicability.

3 Main results

3.1 Fixed-time command filter design

The fixed-time command filter is constructed as

$$\dot{\tilde{\eta}}_{i,j} = -\tau_{1,i,j}\tilde{\eta}_{i,j} - \tau_{2,i,j}\tilde{\eta}_{i,j}^{\alpha} \tanh \frac{\tau_{2,i,j}\tilde{\eta}_{i,j}^{\alpha+1}}{\zeta_{i,j}} - \tau_{3,i,j}\tilde{\eta}_{i,j}^{\beta} \tag{4}$$

with initial condition $\check{\eta}_{i,j}(0) = \eta_{i,j-1}(0)$ for $j = 2, 3, \ldots, \Upsilon_i$. Here $\tilde{\eta}_{i,j} = \check{\eta}_{i,j} - \eta_{i,\,j-1}$ denotes the filtering error, where $\eta_{i,j-1}$ and $\check{\eta}_{i,j}$ denote filter input and output, respectively. Design parameters $\tau_{k,i,j} > 0$ ($k = 1, 2, 3$), and $\zeta_{i,j} > 0$ govern convergence properties.

Lemma 9. *If command filter* (4) *satisfies* $\eta_{i,j}, \dot{\eta}_{i,j} \in \Omega$ *with compact set* Ω *and these signals are continuous, then the filtering error* $\tilde{\eta}_{i,j}$ *converges to a small neighborhood around the origin within fixed time.*

Proof. Consider $W_{i,j} = \tilde{\eta}_{i,j}^2/2$. Its derivative along (4) is

$$\dot{W}_{i,j} = -\tau_{1,i,j}\tilde{\eta}_{i,j}^2 - \tau_{2,i,j}\tilde{\eta}_{i,j}^{\alpha+1}\tanh\frac{\tau_{2,i,j}\tilde{\eta}_{i,j}^{\alpha+1}}{\zeta_{i,j}} - \tau_{3,i,j}\tilde{\eta}_{i,j}^{\beta+1} - \tilde{\eta}_{i,j}\dot{\eta}_{i,j-1}. \tag{5}$$

Applying Lemma 2 to the hyperbolic term yields

$$-\tau_{2,i,j}\tilde{\eta}_{i,j}^{\alpha+1}\tanh\frac{\tau_{2,i,j}\tilde{\eta}_{i,j}^{\alpha+1}}{\zeta_{i,j}} \leqslant -\tau_{2,i,j}\tilde{\eta}_{i,j}^{\alpha+1} + \iota_0\zeta_{i,j}. \tag{6}$$

Using Young's inequality with $|\dot{\eta}_{i,\,j-1}| \leqslant \bar{\eta}_{i,j-1}$ (constant $\bar{\eta}_{i,\,j-1} > 0$), we obtain

$$-\tilde{\eta}_{i,j}\dot{\eta}_{i,j-1} \leqslant \frac{\tau_{1,i,j}}{2}\tilde{\eta}_{i,j}^2 + \frac{1}{2\tau_{1,i,j}}\bar{\eta}_{i,j-1}^2. \tag{7}$$

Substituting (6) and (7) into (5) results in

$$\begin{aligned}\dot{W}_{i,j} &\leqslant -\frac{\tau_{1,i,j}}{2}\tilde{\eta}_{i,j}^2 - \tau_{2,i,j}\tilde{\eta}_{i,j}^{\alpha+1} - \tau_{3,i,j}\tilde{\eta}_{i,j}^{\beta+1} + \tau_{0,i,j}\\ &= -\tau_{1,i,j}W_{i,j} - \bar{\tau}_{2,i,j}W_{i,j}^{(\alpha+1)/2} - \bar{\tau}_{3,i,j}W_{i,j}^{(\beta+1)/2} + \tau_{0,i,j},\end{aligned} \tag{8}$$

where $\bar{\tau}_{2,i,j} = 2^{(\alpha+1)/2}\tau_{2,i,j}$, $\bar{\tau}_{3,i,j} = 2^{(\beta+1)/2}\tau_{3,i,j}$, and $\tau_{0,i,j} = \iota_0\zeta_{i,j} + \bar{\eta}_{i,j-1}^2/2\tau_{1,i,j}$.

Lemma 1 applied to (8) establishes fixed-time convergence

$$\begin{aligned}&|\tilde{\eta}_{i,j}| \leqslant D_{i,j}^1\\ &\quad= \sqrt{2}\min\left\{\sqrt{\frac{\tau_{0,i,j}}{(1-\iota)\tau_{1,i,j}}}, \left(\frac{\tau_{0,i,j}}{(1-\iota)\bar{\tau}_{2,i,j}}\right)^{1/(\alpha+1)}, \left(\frac{\tau_{0,i,j}}{(1-\iota)\bar{\tau}_{3,i,j}}\right)^{1/(\beta+1)}\right\}\end{aligned}$$

for $t \geqslant T_{i,j}^1$, where $0 < \iota < 1$ is a constant, and the settling times satisfy

$$\begin{aligned}&t \leqslant T_{i,j}^1\\ &\quad= 2\max\left\{\frac{\ln(1+\frac{\tau_{1,i,j}}{\iota\bar{\tau}_{2,i,j}})}{\tau_{1,i,j}(1-\alpha)}, \frac{\ln(1+\frac{\iota\tau_{1,i,j}}{\bar{\tau}_{2,i,j}})}{\iota\tau_{1,i,j}(1-\alpha)}\right\} + 2\max\left\{\frac{\ln(1+\frac{\tau_{1,i,j}}{\iota\bar{\tau}_{3,i,j}})}{\tau_{1,i,j}(\beta-1)}, \frac{\ln(1+\frac{\iota\tau_{1,i,j}}{\bar{\tau}_{3,i,j}})}{\iota\tau_{1,i,j}(\beta-1)}\right\}.\end{aligned}$$

The proof is complete. □

Remark 5. The proposed filter (4) extends conventional designs $\dot{\check{\eta}}_{i,j} = -\tau_{1,i,j}\tilde{\eta}_{i,j}$ [1, 6, 19, 21, 28] and $\dot{\check{\eta}}_{i,j} = -\tau_{2,i,j}\tilde{\eta}_{i,j}^{\alpha} - \tau_{3,i,j}\tilde{\eta}_{i,j}^{\beta}$ [10] through enhanced parametric flexibility. Unlike fixed-time filters in [8], formulation (4) eliminates piecewise-continuous components, significantly simplifying stability analysis.

3.2 Error compensation mechanism design

To alleviate the influence of filter errors, the following error compensation mechanism is presented:

$$\begin{aligned}
\dot{s}_{i,1} &= -p_{i,1}s_{i,1} - c_{i,1}s_{i,1}^{\alpha} - d_{i,1}s_{i,1}^{\beta} + \check{g}_{i,1}s_{i,2} + \check{g}_{i,1}\tilde{\eta}_{i,2},\\
\dot{s}_{i,j} &= -p_{i,j}s_{i,j} - c_{i,j}s_{i,j}^{\alpha} - d_{i,j}s_{i,j}^{\beta} - \check{g}_{i,j-1}s_{i,j-1}\\
&\quad + \check{g}_{i,j}s_{i,j+1} + \check{g}_{i,j}\tilde{\eta}_{i,j+1} \quad (j = 2,3,\ldots,\Upsilon_i - 1),\\
\dot{s}_{i,\Upsilon_i} &= -p_{i,\Upsilon_i}s_{i,\Upsilon_i} - c_{i,\Upsilon_i}s_{i,\Upsilon_i}^{\alpha} - d_{i,\Upsilon_i}s_{i,\Upsilon_i}^{\beta} - \check{g}_{i,\Upsilon_i-1}s_{i,\Upsilon_i-1}
\end{aligned} \tag{9}$$

with zero initial states $s_{i,j}(0) = 0$. Design parameters satisfy $p_{i,j} > 0$, $c_{i,j} > 0$, $d_{i,j} > 0$, and gain coefficients $\check{g}_{i,1} = \rho_i g_{i,1}$ with $\rho_i = h_i + b_i$, $\check{g}_{i,j} = g_{i,j}$ for $j = 2,3,\ldots,\Upsilon_i - 1$.

Lemma 10. *System* (9) *achieves PFTS when* $c_{i,j}, d_{i,j} > 1/2$.

Proof. Define the Lyapunov function $W = \sum_{i=1}^{M}\sum_{j=1}^{\Upsilon_i} s_{i,j}^2/2$. Its derivative along (9) satisfies

$$\dot{W} = -\sum_{i=1}^{M}\sum_{j=1}^{\Upsilon_i}\left(p_{i,j}s_{i,j}^2 + c_{i,j}s_{i,j}^{\alpha+1} + d_{i,j}s_{i,j}^{\beta+1}\right) + \sum_{i=1}^{M}\sum_{j=1}^{\Upsilon_i-1}\check{g}_{i,j}s_{i,j}\tilde{\eta}_{i,j+1}. \tag{10}$$

By Lemma 9, after the fixed time $T_{i,j}^1$, the filtering error satisfies $|\tilde{\eta}_{i,j+1}| \leqslant D_{i,j+1}^1$. According to Assumption 2 and Young's inequality, we can further obtain

$$\begin{aligned}
\sum_{i=1}^{M}\sum_{j=1}^{\Upsilon_i-1}\check{g}_{i,j}s_{i,j}\tilde{\eta}_{i,j+1} &\leqslant \sum_{i=1}^{M}\sum_{j=1}^{\Upsilon_i-1}\bar{\check{g}}_{i,j}D_{i,j+1}^1|s_{i,j}|\\
&\leqslant \frac{1}{2}\sum_{i=1}^{M}\sum_{j=1}^{\Upsilon_i-1}\left[s_{i,j}^{\alpha+1} + s_{i,j}^{\beta+1}\right] + \eta_0,
\end{aligned} \tag{11}$$

where $\eta_0 = \sum_{i=1}^{M}\sum_{j=1}^{\Upsilon_i-1}(\bar{\check{g}}_{i,j}D_{i,\,j+1}^1)^2/2$ with $\bar{\check{g}}_{i,1} = \rho_i\bar{g}_{i,1}$ and $\bar{\check{g}}_{i,j} = \bar{g}_{i,j}$ for $j = 2,3,\ldots,\Upsilon_i - 1$.

Substituting (11) into (10) gives

$$\dot{W} \leqslant -\sum_{i=1}^{M}\sum_{j=1}^{\Upsilon_i}\left[p_{i,j}s_{i,j}^2 + \left(c_{i,j} - \frac{1}{2}\right)s_{i,j}^{\alpha+1} + \left(d_{i,j} - \frac{1}{2}\right)s_{i,j}^{\beta+1}\right] + \eta_0. \tag{12}$$

Lemma 3 transforms (12) into

$$\dot{W} \leqslant -p_0W - c_0W^{(\alpha+1)/2} - d_0W^{(\beta+1)/2} + \eta_0,$$

where $p_0 = 2\min\{p_{i,j}\}$, $c_0 = 2^{(\alpha+1)/2}\min\{c_{i,j} - 1/2\}$, and $d_0 = 2^{(\beta+1)/2} \times (\sum_{i=1}^{M}\Upsilon_i)^{(1-\beta]/2}\min\{d_{i,j} - 1/2\}$.

By Lemma 1, system (9) achieves PFTS with the residual set

$$|s_{i,j}| \leqslant D_2 = \sqrt{2}\min\left\{\sqrt{\frac{\eta_0}{(1-\iota)p_0}}, \left(\frac{\eta_0}{(1-\iota)c_0}\right)^{1/(\alpha+1)}, \left(\frac{\eta_0}{(1-\iota)d_0}\right)^{1/(\beta+1)}\right\}, \tag{13}$$

where $0 < \iota < 1$, and the settling time satisfies

$$t \leqslant T_2 = 2\max\left\{\frac{\ln(1+\frac{p_0}{\iota c_0})}{p_0(1-\alpha)}, \frac{\ln(1+\frac{\iota p_0}{c_0})}{\iota p_0(1-\alpha)}\right\} + 2\max\left\{\frac{\ln(1+\frac{p_0}{\iota d_0})}{p_0(\beta-1)}, \frac{\ln(1+\frac{\iota p_0}{d_0})}{\iota p_0(\beta-1)}\right\}. \tag{14}$$

The proof is complete. □

3.3 PFTF control scheme design

Define formation errors $e_{i,1}$, tracking errors $e_{i,j}$ $(j = 2, 3, \ldots, \Upsilon_i)$, and compensated errors $z_{i,j}$ as follows:

$$e_{i,1} = \sum_{j=1}^{M} a_{ij}\big[(y_i - \xi_i) - (y_j - \xi_j)\big] + b_i(y_i - \xi_i - y_r), \tag{15}$$

$$e_{i,j} = x_{i,j} - \check{\eta}_{i,j} \quad (j = 2, 3, \ldots, \Upsilon_i), \tag{16}$$

$$z_{i,j} = e_{i,j} - s_{i,j} \quad (j = 1, 2, \ldots, \Upsilon_i). \tag{17}$$

Then the virtual controllers $\eta_{i,\chi}$, actual controller v_i, and parametric adaptive law $\dot{\hat{\theta}}_i$ are designed as

$$\eta_{i,1} = \frac{1}{\check{g}_{i,1}}\left[\rho_i\dot{\xi}_i + b_i\dot{y}_r - \sum_{j=1}^{M} a_{i,j}\dot{\xi}_j - p_{i,1}e_{i,1} - l_{i,1}z_{i,1}^{\beta} - k_{i,1}z_{i,1}^{\alpha}\tanh\frac{k_{i,1}z_{i,1}^{\alpha+1}}{\varsigma_{i,1}} - \frac{1}{2}(\mu_{i,1}+\nu_{i,1})z_{i,1} - \frac{1}{2\lambda_{i,1}^2}z_{i,1}\hat{\theta}_i\varphi_{i,1}^{\mathrm{T}}(X_{i,1})\varphi_{i,1}(X_{i,1})\right], \tag{18}$$

$$\eta_{i,\chi} = \frac{1}{g_{i,\chi}}\left[\dot{\check{\eta}}_{i,\chi} - \check{g}_{i,\chi-1}e_{i,\chi-1} - p_{i,\chi}e_{i,\chi} - l_{i,\chi}z_{i,\chi}^{\beta} - k_{i,\chi}z_{i,\chi}^{\alpha}\tanh\frac{k_{i,\chi}z_{i,\chi}^{\alpha+1}}{\varsigma_{i,\chi}} - \frac{1}{2}(\mu_{i,\chi}+\nu_{i,\chi})z_{i,\chi} - \frac{1}{2\lambda_{i,\chi}^2}z_{i,\chi}\hat{\theta}_i\varphi_{i,\chi}^{\mathrm{T}}(X_{i,\chi})\varphi_{i,\chi}(X_{i,\chi})\right] \tag{19}$$

for $\chi = 2, \ldots, \Upsilon_i - 1$, and

$$v_i = \frac{N(\vartheta_i)\bar{v}_i}{g_{i,\Upsilon_i}} \tag{20}$$

with

$$\bar{v}_i = -\dot{\bar{\eta}}_{i,\Upsilon_i} + g_{i,\Upsilon_i-1}e_{i,\Upsilon_i-1} + p_{i,\Upsilon_i}e_{i,\Upsilon_i} + k_{i,\Upsilon_i}z_{i,\Upsilon_i}^{\alpha}\tanh\frac{k_{i,\Upsilon_i}z_{i,\Upsilon_i}^{\alpha+1}}{\varsigma_{i,\Upsilon_i}} + l_{i,\Upsilon_i}z_{i,\Upsilon_i}^{\beta} + \frac{1}{2}(\mu_{i,\Upsilon_i}+\nu_{i,\Upsilon_i}+\kappa_i)z_{i,\Upsilon_i} + \frac{1}{2\lambda_{i,\Upsilon_i}^2}z_{i,\Upsilon_i}\hat{\theta}_i\varphi_{i,\Upsilon_i}^{\mathrm{T}}(X_{i,\Upsilon_i})\varphi_{i,\Upsilon_i}(X_{i,\Upsilon_i}).$$

Here $N(\vartheta_i)$ is a Nussbaum-type function [31] with $\dot{\vartheta}_i = z_{i,\Upsilon_i}\bar{v}_i$,

$$\dot{\hat{\theta}}_i = \sum_{j=1}^{\Upsilon_i}\frac{r_i}{2\lambda_{i,j}^2}z_{i,j}^2\varphi_{i,j}^{\mathrm{T}}(X_{i,j})\varphi_{i,j}(X_{i,j}) - w_{i,1}\hat{\theta}_i - w_{i,2}\hat{\theta}_i^{\alpha} - w_{i,3}\hat{\theta}_i^{\beta}, \quad \hat{\theta}_i(t_0)\geqslant 0, \tag{21}$$

where $p_{i,j}$, $k_{i,j}$, $l_{i,j}$, $\lambda_{i,j}$, $\mu_{i,j}$, $\nu_{i,j}$, $\varsigma_{i,j}$, κ_i, r_i, $w_{i,1}$, $w_{i,2}$, and $w_{i,3}$ are all positive design parameters. $\varphi_{i,j}(X_{i,j})$ are the basis function vectors of NNs with $X_{i,1} = [x_{i,1}, x_{j,1}, s_{i,1}]^{\mathrm{T}}$ $(j\in\{j \mid a_{i,j}=1\})$ and $X_{i,j} = [\bar{x}_{i,j}, s_{i,j}]^{\mathrm{T}} (j = 2,3,\ldots,\Upsilon_i)$.

Theorem 1. *For MASs* (1)*, reference signal* y_r*, and formation information* ξ*, under Assumptions* 1–5*, the PFTF of MAS* (1) *can be achieved by using the fixed-time command filter* (4)*, fixed-time error compensation mechanism* (9)*, virtual controllers* (18) *and* (19)*, actual controller* (20)*, and parametric adaptive law* (21)*.*

Proof. Employ backstepping technique [22].

Step $i,1$. Define

$$V_{i,1} = \frac{1}{2}z_{i,1}^2.$$

Its derivative along (1), (15), and (17) trajectories is

$$\dot{V}_{i,1} = z_{i,1}\Bigg[\rho_i\big(g_{i,1}x_{i,2} + f_{i,1} + \omega_{i,1} - \dot{\xi}_i\big) - b_i\dot{y}_r - \sum_{j=1}^{M}a_{i,j}\big(g_{j,1}x_{j,2} + f_{j,1} + \omega_{j,1} - \dot{\xi}_j\big) - \dot{s}_{i,1}\Bigg]. \tag{22}$$

Incorporating (9), (22) can be rewritten as

$$\dot{V}_{i,1} = z_{i,1}\Bigg[\check{g}_{i,1}z_{i,2} + \check{g}_{i,1}\eta_{i,1} - \rho_i\dot{\xi}_i - b_i\dot{y}_r + \sum_{j=1}^{M}a_{i,j}\dot{\xi}_j + p_{i,1}s_{i,1} + F_{i,1}(\bar{X}_{i,1}) + \rho_i\omega_{i,1} - \sum_{j=1}^{M}a_{i,j}\omega_{j,1}\Bigg], \tag{23}$$

where

$$F_{i,1}(\bar{X}_{i,1}) = \rho_i f_{i,1} - \sum_{j=1}^{M}a_{i,j}(g_{j,1}x_{j,2} + f_{j,1}) + c_{i,1}s_{i,1}^{\alpha} + d_{i,1}s_{i,1}^{\beta}$$

and

$$\bar{X}_{i,1} = [x_{i,1}, x_{j,1}, x_{j,2}, s_{i,1}]^{\mathrm{T}} \quad \big(j\in\{j \mid a_{i,j}=1\}\big).$$

By [32], there exists a sufficiently large compact set Ω such that $\bar{X}_{i,1} \in \Omega$. Approximate $F_{i,1}(\bar{X}_{i,1})$ via NNs

$$F_{i,1}(\bar{X}_{i,1}) = \theta_{i,1}^{\mathrm{T}}\varphi_{i,1}(\bar{X}_{i,1}) + \varepsilon_{i,1}(\bar{X}_{i,1}),$$

where the approximation error $\varepsilon_{i,1}(\bar{X}_{i,1})$ satisfies $|\varepsilon_{i,1}(\bar{X}_{i,1})| \leqslant \bar{\varepsilon}_{i,1}$ with $\bar{\varepsilon}_{i,1} > 0$. Applying Young's inequality and Lemma 5, one has

$$\begin{aligned} z_{i,1}F_{i,1}(\bar{X}_{i,1}) \leqslant{}& \frac{1}{2\lambda_{i,1}^2}z_{i,1}^2\|\theta_{i,1}\|^2\varphi_{i,1}^{\mathrm{T}}(X_{i,1})\varphi_{i,1}(X_{i,1}) + \frac{1}{2}\lambda_{i,1}^2 \\ &+ \frac{1}{2}\mu_{i,1}z_{i,1}^2 + \frac{1}{2\mu_{i,1}}\bar{\varepsilon}_{i,1}^2. \end{aligned} \tag{24}$$

Based on Assumption 3, the disturbance term satisfies $|\rho_i\omega_{i,1} - \sum_{j=1}^{M} a_{i,j}\omega_{j,1}| \leqslant \bar{\varpi}_i$, where $\bar{\varpi}_i = \rho_i\bar{\omega}_{i,1} + \sum_{j=1}^{M} a_{i,j}\bar{\omega}_{j,1}$. Reapplying Young's inequality, we have

$$z_{i,1}\left(\rho_i\omega_{i,1} - \sum_{j=1}^{M} a_{i,j}\omega_{j,1}\right) \leqslant \frac{1}{2}\nu_{i,1}z_{i,1}^2 + \frac{1}{2\nu_{i,1}}\bar{\varpi}_i^2. \tag{25}$$

Substituting (24) and (25) into (23), it follows that

$$\begin{aligned} \dot{V}_{i,1} \leqslant{}& z_{i,1}\left(\check{g}_{i,1}z_{i,2} + \check{g}_{i,1}\eta_{i,1} - \rho_i\dot{\xi}_i - b_i\dot{y}_r + \sum_{j=1}^{M} a_{i,j}\dot{\xi}_j + p_{i,1}s_{i,1}\right) \\ &+ \frac{1}{2}(\mu_{i,1} + \nu_{i,1})z_{i,1}^2 + \frac{1}{2\lambda_{i,1}^2}z_{i,1}^2\|\theta_{i,1}\|^2\varphi_{i,1}^{\mathrm{T}}(X_{i,1})\varphi_{i,1}(X_{i,1}) \\ &+ \frac{1}{2}\left(\lambda_{i,1}^2 + \frac{\bar{\varpi}_i^2}{\nu_{i,1}} + \frac{\bar{\varepsilon}_{i,1}^2}{\mu_{i,1}}\right). \end{aligned} \tag{26}$$

Inserting the designed virtual controller (18) into (26) and applying Lemma 2 yields

$$\begin{aligned} \dot{V}_{i,1} \leqslant{}& \check{g}_{i,1}z_{i,1}z_{i,2} - p_{i,1}z_{i,1}^2 - k_{i,1}z_{i,1}^{\alpha+1} - l_{i,1}z_{i,1}^{\beta+1} + \frac{1}{2}\left(\lambda_{i,1}^2 + \frac{\bar{\varpi}_i^2}{\nu_{i,1}} + \frac{\bar{\varepsilon}_{i,1}^2}{\mu_{i,1}}\right) \\ &+ \frac{1}{2\lambda_{i,1}^2}z_{i,1}^2\big(\|\theta_{i,1}\|^2 - \hat{\theta}_i\big)\varphi_{i,1}^{\mathrm{T}}(X_{i,1})\varphi_{i,1}(X_{i,1}) + \iota_0\varsigma_{i,1}. \end{aligned}$$

The proof is complete. □

Remark 6. Fixed-time convergence of filter (4) requires bounded derivatives of virtual controller $\eta_{i,1}$ (Lemma 9). However, incorporating the fractional-power term $z_{i,1}^{\alpha}$ ($0 < \alpha < 1$) introduces a potential singularity issue, as the derivative $\alpha z_{i,1}^{\alpha-1}$ becomes unbounded when $z_{i,1} \to 0$. To address this issue, the $\tanh(\cdot)$ function is introduced in (18). By l'Hospital's rule,

$$\begin{aligned} \lim_{z_{i,1}\to 0} \alpha k_{i,1}z_{i,1}^{\alpha-1}\tanh\frac{k_{i,1}z_{i,1}^{\alpha+1}}{\varsigma_{i,1}} &= \lim_{z_{i,1}\to 0}\frac{\alpha k_{i,1}^2(1+\alpha)}{(1-\alpha)\varsigma_{i,1}}\left[1 - \tanh^2\frac{k_{i,1}z_{i,1}^{\alpha+1}}{\varsigma_{i,1}}\right]z_{i,1}^{2\alpha} \\ &= 0. \end{aligned}$$

This guarantees the elimination of control singularity while preserving the desired convergence properties. Additionally, under Assumptions 2 and 5, $\dot{\eta}_{i,1}$ remains continuous and bounded in compact set Ω [33]. This methodology extends to all subsequent control design steps.

Step i, χ ($\chi = 2, \ldots, \Upsilon_i - 1$). Define

$$V_{i,\chi} = V_{i,\chi-1} + \frac{1}{2} z_{i,\chi}^2.$$

Its derivative along (1), (16), and (17) trajectories is

$$\dot{V}_{i,\chi} = \dot{V}_{i,\chi-1} + z_{i,\chi}(g_{i,\chi} x_{i,\chi+1} + f_{i,\chi} + \omega_{i,\chi} - \dot{\bar{\eta}}_{i,\chi} - \dot{s}_{i,\chi}). \tag{27}$$

Incorporating (9), (27) can be rewritten

$$\begin{aligned} \dot{V}_{i,\chi} = \dot{V}_{i,\chi-1} + z_{i,\chi}\big[& g_{i,\chi} z_{i,\chi+1} + g_{i,\chi}\eta_{i,\chi} - \dot{\bar{\eta}}_{i,\chi} + p_{i,\chi} s_{i,\chi} \\ & + \check{g}_{i,\chi-1} s_{i,\chi-1} + F_{i,\chi}(X_{i,\chi}) + \omega_{i,\chi}\big], \end{aligned} \tag{28}$$

where

$$F_{i,\chi}(X_{i,\chi}) = f_{i,\chi} + c_{i,\chi} s_{i,\chi}^{\alpha} + d_{i,\chi} s_{i,\chi}^{\beta}$$

. Approximate $F_{i,\chi}(X_{i,\chi})$ via NNs

$$F_{i,\chi}(X_{i,\chi}) = \theta_{i,\chi}^{\mathrm{T}} \varphi_{i,\chi}(X_{i,\chi}) + \varepsilon_{i,\chi}(X_{i,\chi}),$$

where the approximation error $\varepsilon_{i,\chi}(X_{i,\chi})$ satisfies $|\varepsilon_{i,\chi}(X_{i,\chi})| \leqslant \bar{\varepsilon}_{i,\chi}$ with $\bar{\varepsilon}_{i,\chi} > 0$. Applying Young's inequality, we can get

$$\begin{aligned} z_{i,\chi} F_{i,\chi}(X_{i,\chi}) \leqslant & \frac{1}{2\lambda_{i,\chi}^2} z_{i,\chi}^2 \|\theta_{i,\chi}\|^2 \varphi_{i,\chi}^{\mathrm{T}}(X_{i,\chi}) \varphi_{i,\chi}(X_{i,\chi}) \\ & + \frac{1}{2}\lambda_{i,\chi}^2 + \frac{1}{2}\mu_{i,\chi} z_{i,\chi}^2 + \frac{1}{2\mu_{i,\chi}} \bar{\varepsilon}_{i,\chi}^2 \end{aligned} \tag{29}$$

and

$$z_{i,\chi}\omega_{i,\chi} \leqslant \frac{1}{2}\nu_{i,\chi} z_{i,\chi}^2 + \frac{1}{2\nu_{i,\chi}} \bar{\omega}_{i,\chi}^2. \tag{30}$$

Substituting (29) and (30) into (28), we obtain

$$\begin{aligned} \dot{V}_{i,\chi} \leqslant & \dot{V}_{i,\chi-1} + z_{i,\chi}(g_{i,\chi} z_{i,\chi+1} + g_{i,\chi}\eta_{i,\chi} - \dot{\check{\eta}}_{i,\chi} + p_{i,\chi} s_{i,\chi} + \check{g}_{i,\chi-1} s_{i,\chi-1}) \\ & + \frac{1}{2}(\mu_{i,\chi} + \nu_{i,\chi}) z_{i,\chi}^2 + \frac{1}{2\lambda_{i,\chi}^2} z_{i,\chi}^2 \|\theta_{i,\chi}\|^2 \varphi_{i,\chi}^{\mathrm{T}}(X_{i,\chi}) \varphi_{i,\chi}(X_{i,\chi}) \\ & + \frac{1}{2}\left(\lambda_{i,\chi}^2 + \frac{\bar{\omega}_{i,\chi}^2}{\nu_{i,\chi}} + \frac{\bar{\varepsilon}_{i,\chi}^2}{\mu_{i,\chi}}\right). \end{aligned} \tag{31}$$

Inserting the designed virtual controller (19) into (31) and applying Lemma 2 yields

$$\begin{aligned}\dot{V}_{i,\chi} \leqslant{}& g_{i,\chi} z_{i,\chi} z_{i,\chi+1} - \sum_{j=1}^{\chi} \left(p_{i,j} z_{i,j}^2 + k_{i,j} z_{i,j}^{\alpha+1} + l_{i,j} z_{i,j}^{\beta+1}\right) \\ &+ \sum_{j=1}^{\chi} \frac{1}{2\lambda_{i,j}^2} z_{i,j}^2 \left(\|\theta_{i,j}\|^2 - \hat{\theta}_i\right) \varphi_{i,j}^{\mathrm{T}}(X_{i,j}) \varphi_{i,j}(X_{i,j}) \\ &+ \frac{1}{2}\left[\frac{\bar{\varpi}_i^2}{\nu_{i,1}} + \sum_{j=2}^{\chi} \frac{\bar{\omega}_{i,j}^2}{\nu_{i,j}} + \sum_{j=1}^{\chi} \left(2\iota_0 \varsigma_{i,j} + \lambda_{i,j}^2 + \frac{\bar{\varepsilon}_{i,j}^2}{\mu_{i,j}}\right)\right].\end{aligned}$$

Step i, Υ_i. Define

$$V_{i,\Upsilon_i} = V_{i,\Upsilon_i - 1} + \frac{1}{2} z_{i,\Upsilon_i}^2.$$

Its derivative along (1), (16), and (17) trajectories is

$$\begin{aligned}\dot{V}_{i,\Upsilon_i} = \dot{V}_{i,\Upsilon_i - 1} + z_{i,\Upsilon_i}\big(&g_{i,\Upsilon_i} u_i(v_i) + \omega_{i,\Upsilon_i} - \dot{\bar{\eta}}_{i,\Upsilon_i} - \dot{s}_{i,\Upsilon_i} \\ &+ g_{i,\Upsilon_i} J_i(t - \tau_i) \Pi_i(\bar{x}_{i,\Upsilon_i}, u_i) + f_{i,\Upsilon_i}\big).\end{aligned} \tag{32}$$

By Assumption 4 and Young's inequality, we have

$$\begin{aligned}&z_{i,\Upsilon_i}\left(g_{i,\Upsilon_i} J_i(t - \tau_i) \Pi_i(\bar{x}_{i,\Upsilon_i}, u_i) + f_{i,\Upsilon_i}\right) \\ &\quad\leqslant |z_{i,\Upsilon_i}| \bar{f}_{i,\Upsilon_i}(\bar{x}_{i,\Upsilon_i}, u_i) \leqslant \frac{1}{2\jmath_i} z_{i,\Upsilon_i}^2 \bar{f}_{i,\Upsilon_i}^2(\bar{x}_{i,\Upsilon_i}, u_i) + \frac{1}{2}\jmath_i,\end{aligned}$$

where $\jmath_i > 0$ is a design parameter. Combining with (2) and (9), (32) can be bounded as

$$\begin{aligned}\dot{V}_{i,\Upsilon_i} \leqslant \dot{V}_{i,\Upsilon_i - 1} + z_{i,\Upsilon_i}\big[&g_{i,\Upsilon_i} h_i v_i - \dot{\bar{\eta}}_{i,\Upsilon_i} + p_{i,\Upsilon_i} s_{i,\Upsilon_i} + \omega_{i,\Upsilon_i} \\ &+ g_{i,\Upsilon_i - 1} s_{i,\Upsilon_i - 1} + F_{i,\Upsilon_i}(X_{i,\Upsilon_i}, u_i) + g_{i,\Upsilon_i}\sigma_i\big] + \frac{1}{2}\jmath_i,\end{aligned} \tag{33}$$

where

$$F_{i,\Upsilon_i}(X_{i,\Upsilon_i}, u_i) = \frac{1}{2\jmath_i} z_{i,\Upsilon_i} \bar{f}_{i,\Upsilon_i}^2(\bar{x}_{i,\Upsilon_i}, u_i) + c_{i,\Upsilon_i} s_{i,\Upsilon_i}^{\alpha} + d_{i,\Upsilon_i} s_{i,\Upsilon_i}^{\beta}.$$

Approximate $F_{i,\Upsilon_i}(X_{i,\Upsilon_i}, u_i)$ via NNs

$$F_{i,\Upsilon_i}(X_{i,\Upsilon_i}, u_i) = \theta_{i,\Upsilon_i}^{\mathrm{T}} \varphi_{i,\Upsilon_i}(X_{i,\Upsilon_i}, u_i) + \varepsilon_{i,\Upsilon_i}(X_{i,\Upsilon_i}, u_i),$$

where $|\varepsilon_{i,\Upsilon_i}(X_{i,\Upsilon_i}, u_i)| \leqslant \bar{\varepsilon}_{i,\Upsilon_i}$ with $\bar{\varepsilon}_{i,\Upsilon_i} > 0$. Applying Young's inequality and Lemma 5 yields

$$\begin{aligned}z_{i,\Upsilon_i} F_{i,\Upsilon_i}(X_{i,\Upsilon_i}, u_i) \leqslant{}& \frac{1}{2\lambda_{i,\Upsilon_i}^2} z_{i,\Upsilon_i}^2 \|\theta_{i,\Upsilon_i}\|^2 \varphi_{i,\Upsilon_i}^{\mathrm{T}}(X_{i,\Upsilon_i}) \varphi_{i,\Upsilon_i}(X_{i,\Upsilon_i}) \\ &+ \frac{1}{2}\lambda_{i,\Upsilon_i}^2 + \frac{1}{2}\mu_{i,\Upsilon_i} z_{i,\Upsilon_i}^2 + \frac{1}{2\mu_{i,\Upsilon_i}} \bar{\varepsilon}_{i,\Upsilon_i}^2,\end{aligned} \tag{34}$$

$$z_{i,\Upsilon_i}\omega_{i,\Upsilon_i} \leqslant \frac{1}{2}\nu_{i,\Upsilon_i}z_{i,\Upsilon_i}^2 + \frac{1}{2\nu_{i,\Upsilon_i}}\bar{\omega}_{i,\Upsilon_i}^2,$$

and

$$z_{i,\Upsilon_i}g_{i,\Upsilon_i}\sigma_i \leqslant \frac{1}{2}\kappa_i z_{i,\Upsilon_i}^2 + \frac{1}{2\kappa_i}\bar{g}_{i,\Upsilon_i}^2\bar{\sigma}_i^2. \tag{35}$$

Substituting (34)–(35) into (33), it follows that

$$\begin{aligned}\dot{V}_{i,\Upsilon_i} \leqslant{}& \dot{V}_{i,\Upsilon_i-1} + z_{i,\Upsilon_i}\big(g_{i,\Upsilon_i}h_i v_i - \dot{\bar{\eta}}_{i,\Upsilon_i} + p_{i,\Upsilon_i}s_{i,\Upsilon_i} + g_{i,\Upsilon_i-1}s_{i,\Upsilon_i-1}\big)\\ &+ \frac{1}{2}(\mu_{i,\Upsilon_i} + \nu_{i,\Upsilon_i} + \kappa_i)z_{i,\Upsilon_i}^2\\ &+ \frac{1}{2\lambda_{i,\Upsilon_i}^2}z_{i,\Upsilon_i}^2\|\theta_{i,\Upsilon_i}\|^2\varphi_{i,\Upsilon_i}^{\mathrm{T}}(X_{i,\Upsilon_i})\varphi_{i,\Upsilon_i}(X_{i,\Upsilon_i})\\ &+ \frac{1}{2}\left(\jmath_i + \lambda_{i,\Upsilon_i}^2 + \frac{\bar{\omega}_{i,\Upsilon_i}^2}{\nu_{i,\Upsilon_i}} + \frac{\bar{\varepsilon}_{i,\Upsilon_i}^2}{\mu_{i,\Upsilon_i}} + \frac{\bar{g}_{i,\Upsilon_i}^2\bar{\sigma}_i^2}{\kappa_i}\right).\end{aligned} \tag{36}$$

Remark 7. Controller design exploits Lemma 5 to derive the critical inequality

$$\varphi_{i,\Upsilon_i}^{\mathrm{T}}(X_{i,\Upsilon_i},u_i)\varphi_{i,\Upsilon_i}(X_{i,\Upsilon_i},u_i) \leqslant \varphi_{i,\Upsilon_i}^{\mathrm{T}}(X_{i,\Upsilon_i})\varphi_{i,\Upsilon_i}(X_{i,\Upsilon_i}).$$

Direct incorporation of $\varphi_{i,\Upsilon_i}(X_{i,\Upsilon_i},u_i)$ into controller (20) would induce an algebraic loop [21]. Existing methods [3, 17] necessitate Butterworth filters to resolve this issue. The inequality-based solution in (34) circumvents the algebraic loop by leveraging inherent properties of basis functions, significantly simplifying implementation.

Inserting the designed actual controller (20) into (36) results in

$$\begin{aligned}\dot{V}_{i,\Upsilon_i} \leqslant{}& \big(h_i N(\vartheta_i)+1\big)\dot{\vartheta}_i + \Delta_{1,i} - \sum_{j=1}^{\Upsilon_i}\big(p_{i,j}z_{i,j}^2 + k_{i,j}z_{i,j}^{\alpha+1} + l_{i,j}z_{i,j}^{\beta+1}\big)\\ &+ \sum_{j=1}^{\Upsilon_i}\frac{1}{2\lambda_{i,j}^2}z_{i,j}^2\big(\|\theta_{i,j}\|^2 - \hat{\theta}_i\big)\varphi_{i,j}^{\mathrm{T}}(X_{i,j})\varphi_{i,j}(X_{i,j}),\end{aligned} \tag{37}$$

where

$$\Delta_{1,i} = \frac{1}{2}\left[\jmath_i + \frac{\bar{\varpi}_i^2}{\nu_{i,1}} + \sum_{j=2}^{\Upsilon_i}\left(2\iota_0\varsigma_{i,j-1} + \frac{\bar{\omega}_{i,j}^2}{\nu_{i,j}}\right) + \sum_{j=1}^{\Upsilon_i}\left(\lambda_{i,j}^2 + \frac{\bar{\varepsilon}_{i,j}^2}{\mu_{i,j}}\right) + \frac{\bar{g}_{i,\Upsilon_i}^2\bar{\sigma}_i^2}{\kappa_i}\right].$$

Define $\theta_i = \max_{1\leqslant j\leqslant\Upsilon_i}\{\|\theta_{i,j}\|^2\}$, the parametric adaptive law $\dot{\hat{\theta}}_i$ is constructed as (21). Introduce the composite Lyapunov function

$$V_i = V_{i,\Upsilon_i} + \frac{1}{2r_i}\tilde{\theta}_i^2, \tag{38}$$

where $\tilde{\theta}_i = \theta_i - \hat{\theta}_i$. Combining (21), (37), and (38), we have

$$\begin{aligned}\dot{V}_i &= \dot{V}_{i,\Upsilon_i} - \frac{1}{r_i}\tilde{\theta}_i\dot{\hat{\theta}}_i \\ &\leqslant \big(h_i N(\vartheta_i)+1\big)\dot{\vartheta}_i - \sum_{j=1}^{\Upsilon_i}\big(p_{i,j}z_{i,j}^2 + k_{i,j}z_{i,j}^{\alpha+1} + l_{i,j}z_{i,j}^{\beta+1}\big) \\ &\quad + \frac{w_{i,1}}{r_i}\tilde{\theta}_i\hat{\theta}_i + \frac{w_{i,2}}{r_i}\tilde{\theta}_i\hat{\theta}_i^{\alpha} + \frac{w_{i,3}}{r_i}\tilde{\theta}_i\hat{\theta}_i^{\beta} + \Delta_{1,i}. \end{aligned} \tag{39}$$

Applying Young's inequality, it yields

$$\tilde{\theta}_i\hat{\theta}_i \leqslant \frac{1}{2}\big(-\tilde{\theta}_i^2 + \theta_i^2\big). \tag{40}$$

From (21) and noting that $\hat{\theta}_i(t_0) \geqslant 0$, we apply Lemma 8 to conclude that $\hat{\theta}_i(t) \geqslant 0$ holds for all $t \geqslant 0$. Furthermore, by applying Lemma 6, we obtain

$$\tilde{\theta}_i\hat{\theta}_i^{\alpha} = (\theta_i - \hat{\theta}_i)\hat{\theta}_i^{\alpha} \leqslant \frac{1}{\alpha+1}\big(\theta_i^{\alpha+1} - \hat{\theta}_i^{\alpha+1}\big)$$

and

$$\hat{\theta}_i^{\alpha+1} = (\theta_i - \tilde{\theta}_i)^{\alpha+1} \geqslant \tilde{\theta}_i^{\alpha+1} - \theta_i^{\alpha+1}.$$

By combining the two inequalities above, we can deduce that

$$\tilde{\theta}_i\hat{\theta}_i^{\alpha} \leqslant \frac{1}{\alpha+1}\big(-\tilde{\theta}_i^{\alpha+1} + 2\theta_i^{\alpha+1}\big). \tag{41}$$

Similarly, we can also obtain that

$$\tilde{\theta}_i\hat{\theta}_i^{\beta} \leqslant \frac{1}{\beta+1}\big(-\tilde{\theta}_i^{\beta+1} + 2\theta_i^{\beta+1}\big). \tag{42}$$

Substituting (40)–(42) into (39) yields

$$\begin{aligned}\dot{V}_i &\leqslant \big(h_i N(\vartheta_i)+1\big)\dot{\vartheta}_i - \sum_{j=1}^{\Upsilon_i}\big(p_{i,j}z_{i,j}^2 + k_{i,j}z_{i,j}^{\alpha+1} + l_{i,j}z_{i,j}^{\beta+1}\big) \\ &\quad - \frac{w_{i,1}}{2r_i}\tilde{\theta}_i^2 - \frac{w_{i,2}}{(\alpha+1)r_i}\tilde{\theta}_i^{\alpha+1} - \frac{w_{i,3}}{(\beta+1)r_i}\tilde{\theta}_i^{\beta+1} + \Delta_{2,i}, \end{aligned} \tag{43}$$

where

$$\Delta_{2,i} = \Delta_{1,i} + \frac{w_{i,1}}{2r_i}\theta_i^2 + \frac{2w_{i,2}}{(\alpha+1)r_i}\theta_i^{\alpha+1} + \frac{2w_{i,3}}{(\beta+1)r_i}\theta_i^{\beta+1}.$$

Finally, the total Lyapunov function V is chosen as

$$V = \sum_{i=1}^{M} V_i, \tag{44}$$

where V_i is given by (38). Combining (43), (44), and Lemma 3, we derive

$$\begin{aligned}\dot{V} \leqslant & -\sum_{i=1}^{M}\left[\left(\sum_{j=1}^{\Upsilon_i} p_{i,j} z_{i,j}^2\right) + \frac{w_{i,1}}{2r_i}\tilde{\theta}_i^2\right] - \sum_{i=1}^{M}\left[\left(\sum_{j=1}^{\Upsilon_i} k_{i,j} z_{i,j}^{\alpha+1}\right) + \frac{w_{i,2}}{(\alpha+1)r_i}\tilde{\theta}_i^{\alpha+1}\right] \\ & - \sum_{i=1}^{M}\left[\left(\sum_{j=1}^{\Upsilon_i} l_{i,j} z_{i,j}^{\beta+1}\right) + \frac{w_{i,3}}{(\beta+1)r_i}\tilde{\theta}_i^{\beta+1}\right] + \sum_{i=1}^{M}\big(h_i N(\vartheta_i)+1\big)\dot{\vartheta}_i + \sum_{i=1}^{M}\Delta_{2,i} \\ \leqslant & -q_0 V - k_0 V^{(\alpha+1)/2} - l_0 V^{(\beta+1)/2} + \sum_{i=1}^{M}\big(h_i N(\vartheta_i)+1\big)\dot{\vartheta}_i + \Delta_2, \end{aligned} \tag{45}$$

where

$$\Delta_2 = \sum_{i=1}^{M}\Delta_{2,i}, \qquad q_0 = \min\{2p_{i,j}, w_{i,1}\},$$

$$k_0 = 2^{(\alpha+1)/2}\min\left\{k_{i,j}, \frac{w_{i,2} r_i^{(\alpha-1)/2}}{\alpha+1}\right\},$$

$$l_0 = 2^{(\beta+1)/2}\left(M + \sum_{i=1}^{M}\Upsilon_i\right)^{(1-\beta)/2}\min\left\{l_{i,j}, \frac{w_{i,3} r_i^{(\beta-1)/2}}{\beta+1}\right\}.$$

By Lemma 7, V and ϑ_i remain bounded. This implies boundedness of $z_{i,j}$ and $\tilde{\theta}_i$, consequently $\hat{\theta}_i$ is bounded. Lemmas 9 and 10 guarantee bounded $\dot{\bar{\eta}}_{i,j}$ and $s_{i,j}$. Since $e_{i,j} = z_{i,j} + s_{i,j}$, $e_{i,j}$ remains bounded. The boundedness of $z_{i,j}$, $\dot{\bar{\eta}}_{i,j}$, $e_{i,j}$, ϑ_i, $\hat{\theta}_i$ combined with controllers (18)–(20) ensures that $\eta_{i,j}$, v_i, and $\dot{\vartheta}_i$ are bounded. Furthermore, from Assumption 2 and the boundedness of ϑ_i and $\dot{\vartheta}_i$ one can conclude that $\sum_{i=1}^{M}(h_i N(\vartheta_i)+1)\dot{\vartheta}_i$ is bounded. Thus, let

$$\left|\sum_{i=1}^{M}\big(h_i N(\vartheta_i)+1\big)\dot{\vartheta}_i\right| \leqslant \Delta_3, \tag{46}$$

where $\Delta_3 > 0$ is a constant.

Substituting (46) into (45) gives

$$\dot{V} \leqslant -q_0 V - k_0 V^{(\alpha+1)/2} - l_0 V^{(\beta+1)/2} + \Delta$$

with $\Delta = \Delta_2 + \Delta_3$. Lemma 1 ensures that $z_{i,j}$ and $\tilde{\theta}_i/\sqrt{r_i}$ converge to

$$D_3 = \sqrt{2}\min\left\{\sqrt{\frac{\Delta}{(1-\iota)q_0}}, \left(\frac{\Delta}{(1-\iota)k_0}\right)^{1/(\alpha+1)}, \left(\frac{\Delta}{(1-\iota)l_0}\right)^{1/(\beta+1)}\right\}, \tag{47}$$

where $0 < \iota < 1$, and the settling time is bounded by

$$\begin{aligned} t &\leqslant T_3 \\ &= 2\max\left\{\frac{\ln(1+\frac{q_0}{\iota k_0})}{q_0(1-\alpha)}, \frac{\ln(1+\frac{\iota q_0}{k_0})}{\iota q_0(1-\alpha)}\right\} + 2\max\left\{\frac{\ln(1+\frac{q_0}{\iota l_0})}{q_0(\beta-1)}, \frac{\ln(1+\frac{\iota q_0}{l_0})}{\iota q_0(\beta-1)}\right\}. \end{aligned} \tag{48}$$

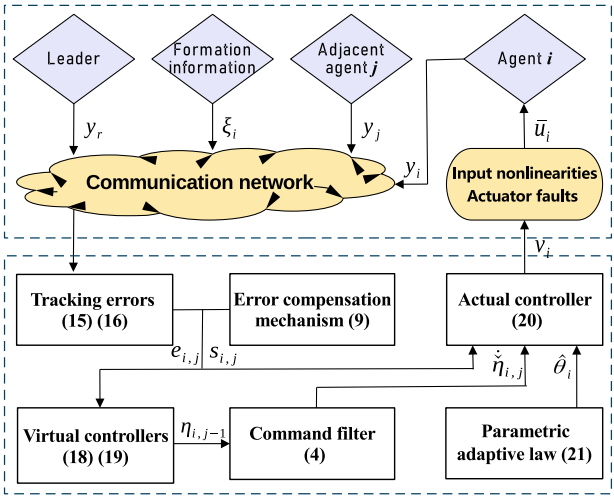

Figure 1. Control block diagram.

Finally, define $\Gamma = [e_{1,1}, e_{2,1}, \ldots, e_{M,1}]^{\mathrm{T}}$, $\Xi = [y_1 - \xi_1 - y_r,\ y_2 - \xi_2 - y_r,\ \ldots,\ y_M - \xi_M - y_r]^{\mathrm{T}}$. From (15) $\Gamma = (L + B)\Xi$. Define $s_1 = [s_{1,1}, s_{2,1}, \ldots, s_{M,1}]^{\mathrm{T}}$ and $z_1 = [z_{1,1}, z_{2,1}, \ldots, z_{M,1}]^{\mathrm{T}}$. Based on (13) and (47), it is derived that $\|s_1\| \leqslant D_2$ and $\|z_1\| \leqslant D_3$ for $t \geqslant T = \max\{T_{i,j}^1\} + T_2 + T_3$. Combining with (17), one further has

$$\begin{aligned} |y_i - \xi_i - y_r| &\leqslant \|\Xi\| \leqslant \left\|(L + B)^{-1}\right\| \|s_1 + z_1\| \\ &\leqslant \left\|(L + B)^{-1}\right\| (D_2 + D_3) = \delta \quad (i = 1, 2, \ldots, M). \end{aligned} \tag{49}$$

To enhance the intuitiveness and clarity of the entire control scheme, the control block diagram is depicted in Fig. 1.

Remark 8. Theorem 1 reveals that design parameters critically govern the formation error bound δ and settling time bound T. These performance metrics are tunable through parameter adjustment. For instance, (49) indicates that sufficiently small δ requires minimization of D_2 and D_3. With fixed $\lambda_{i,j}$, $\mu_{i,j}$, $\nu_{i,j}$, $\varsigma_{i,j}$, κ_i, $w_{i,1}$, $w_{i,2}$, and $w_{i,3}$, parameter selection follows these guidelines: increase $p_{i,j}$, $c_{i,j}$, and $d_{i,j}$ to reduce D_2 via (13); enlarge $k_{i,j}$, $l_{i,j}$, and r_i to diminish D_3 through (47). This approach concurrently shortens convergence time as evidenced by (14) and (48). However, (20) reveals that such parameter escalation amplifies control inputs, elevating operational costs. Practical implementation thus necessitates adjusting these parameters through a trial-and-error method.

Remark 9. Theorem 1 presents a novel PFTF protocol for MASs described by (1). This framework systematically addresses a variety of heterogeneous factors in a holistic manner. Unlike asymptotic formation approaches, our strategy's settling time bound T remains independent of initial conditions. Crucially, diverging from finite-time and fixed-time methods, our scheme employs Lemma 1's stability criterion

$$\dot{W}(\Gamma) \leqslant -\gamma_1 W(\Gamma) - \gamma_2 W^{\Delta_1}(\Gamma) - \gamma_3 W^{\Delta_2}(\Gamma) + \gamma_0,$$

where $\gamma_i > 0$ $(i = 0, 1, 2, 3)$, $0 < \Delta_1 < 1$, and $\Delta_2 > 1$. This triple-exponential structure regulates convergence more effectively than finite-time inequalities $\dot{W}(\Gamma) \leqslant -\gamma_2 W^{\Delta_1}(\Gamma) + \gamma_0$ [6, 13, 21, 27] or $\dot{W}(\Gamma) \leqslant -\gamma_1 W(\Gamma) - \gamma_2 W^{\Delta_1}(\Gamma) + \gamma_0$ [3, 24, 33], and fixed-time inequality $\dot{W}(\Gamma) \leqslant -\gamma_2 W^{\Delta_1}(\Gamma) - \gamma_3 W^{\Delta_2}(\Gamma) + \gamma_0$ [4, 8, 11, 14, 23, 25]. The inclusion of the additional exponential term enhances parameter selection flexibility and has the potential to improve convergence speed and system performance.

Remark 10. PFTF control research confronts substantial challenges from coexisting input nonlinearities, actuator faults, and triple-exponential stability terms. Our solution transforms input nonlinearities into unknown direction problems resolved via Nussbaum functions. Nonaffine actuator faults are mitigated through basis function vector properties. A holistic methodology integrating command filters, error compensation mechanisms, and controllers is adopted. Moreover, the fixed-time stability analysis with three exponential terms is achieved via inequality techniques. Among them, the parametric adaptive law (21) incorporates the three exponential terms of $\hat{\theta}_i$, which poses difficulties for stability analysis. We ensure the nonnegativity of the adaptive parameter $\hat{\theta}_i$ by means of the newly introduced Lemma 8, and on this basis, Young's inequality and Lemma 6 are utilized to handle these three exponential terms (see Eqs. (40)–(42)). Thereby, the technical challenge in the PFTS analysis of the entire system is successfully resolved.

4 Simulation

Example. This example addresses the PFTF control problem for a multiship system. Based on the ship dynamics presented in [19], the Nomoto model for each vessel is formulated as

$$\ddot{\varpi}_i + \frac{R_i}{K_i} M(\dot{\varpi}_i) = u_i,$$

where ϖ_i and $\dot{\varpi}_i$ denote the heading angle and angular rate of the ship, respectively. The parameter K_i represents the ratio of moment of inertia to damping moment, R_i is the ratio of rudder torque to damping moment, and $(K_i/R_i)u_i$ corresponds to the rudder angle. Here $M(\dot{\varpi}_i) = b_{i,1}\dot{\varpi}_i + b_{i,2}\dot{\varpi}_i^3$ with $b_{i,1}$ and $b_{i,2}$ being constant coefficients. Defining state variables $\dot{x}_{i,1} = \varpi_i$ and $x_{i,2} = \dot{\varpi}_i$ and incorporating input nonlinearity $u_i(v_i(t))$, nonaffine actuator fault $J_i(t - \tau_i)\Pi_i(x_{i,1}, x_{i,2}, u_i)$, unmodeled dynamics $f_{i,1}(x_{i,1})$ and $f_{i,2}(x_{i,1}, x_{i,2})$, and unknown disturbances $\omega_{i,1}$ and $\omega_{i,2}$, the Nomoto model is reformulated into the state-space form

$$\begin{aligned}
\dot{x}_{i,1} &= x_{i,2} + f_{i,1}(x_{i,1}) + \omega_{i,1}, \\
\dot{x}_{i,2} &= \bar{u}_i - \frac{R_i}{K_i}\big(b_{i,1}x_{i,2} + b_{i,2}x_{i,2}^3\big) + f_{i,2}(x_{i,1}, x_{i,2}) + \omega_{i,2}, \\
\bar{u}_i &= u_i\big(v_i(t)\big) + J_i(t - \tau_i)\Pi_i(x_{i,1}, x_{i,2}, u_i).
\end{aligned} \tag{50}$$

A multiship system comprising four followers (labeled 1–4) and one leader (labeled 0) is considered, with the communication topology depicted in Fig. 2.

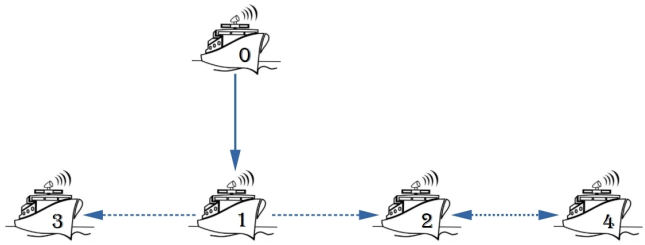

Figure 2. Communication topology of the multiship system.

The follower ships ($i = 1, 2, 3, 4$) adopt the dynamics described by (50). The physical parameters are set as $R_i = K_i = b_{i,1} = b_{i,2} = 1$. Unmodeled dynamics are defined by $f_{i,1}(x_{i,1}) = -0.2x_{i,1}\cos(x_{i,1})$ and $f_{i,2}(x_{i,1}, x_{i,2}) = 2\sin(x_{i,1} - x_{i,2})$. External disturbances are given by $\omega_{i,1} = 0.25\cos(t)$ and $\omega_{i,2} = 0.5\sin(t)$. The control inputs u_i exhibit saturation characteristics defined as

$$u_i = \begin{cases} 15i, & v_i \geqslant 15i, \\ v_i, & -15i < v_i < 15i \ (i = 1, 2, 3, 4), \\ -15i, & v_i \leqslant -15i. \end{cases}$$

The nonaffine actuator fault is characterized by $J_i(t - \tau_i)\Pi_i(x_{i,1}, x_{i,2}, u_i)$. The fault activation function is

$$J_i(t - \tau_i) = \begin{cases} 0, & 0 \leqslant t < 15, \\ 1 - \mathrm{e}^{-50(t-15)}, & t \geqslant 15, \end{cases}$$

and the nonlinear fault profile is $\Pi_i(x_{i,1}, x_{i,2}, u_i) = 2\cos(x_{i,1} - x_{i,2}^2 + u_i)$.

The output of each follower is $y_i = x_{i,1}$, while the leader's output trajectory is $y_r = \sin(0.5t)$. The desired formation configuration is specified by the time-varying vector $\xi = [1,\ 2.5 + 0.5\sin(0.2t),\ -0.5,\ -1.75 - 0.25\sin(0.2t)]$. Key parameters are selected as follows: convergence exponents $\alpha = 3/5$, $\beta = 5/3$; command filter parameters $\tau_{1,i,2} = 1$, $\tau_{2,i,2} = 1$, $\tau_{3,i,2} = 20$, $\zeta_{i,2} = 0.1$; error compensation gains $p_{i,j} = 25$, $c_{i,j} = 1$, $d_{i,j} = 1$; and control parameters $k_{i,j} = 2$, $l_{i,j} = 2$, $\lambda_{i,j} = 40$, $\mu_{i,j} = 2$, $\nu_{i,j} = 2$, $\varsigma_{i,j} = 0.1$, $\jmath_i = 0.1$, $\kappa_i = 2$, $r_i = 20$, $w_{i,j} = 20$. The Nussbaum function is selected as $N(\vartheta_i) = \mathrm{e}^{\vartheta_i^2}\sin(\pi\vartheta_i)$. Initial conditions are $[x_{1,1}(0), x_{1,2}(0)] = [-10, 4.2]$, $[x_{2,1}(0), x_{2,2}(0)] = [3.5, -4.2]$, $[x_{3,1}(0), x_{3,2}(0)] = [-2.8, -3.8]$, $[x_{4,1}(0),\ x_{4,2}(0)] = [8.5, -0.6]$ with parameter estimates initialized to $\hat{\theta}_1(0) = 0.5$, $\hat{\theta}_2(0) = 1$, $\hat{\theta}_3(0) = 1.5$, $\hat{\theta}_4(0) = 2$. All NNs employed in the implementation utilize nine nodes with a width $l_i = \sqrt{2}$ and centers uniformly distributed over $[-4, 4]$.

Simulation results in Figs. 3–8 validate the efficacy of the proposed PFTF control scheme. Figure 3 depicts the follower outputs y_i and the reference trajectory y_r. Figure 4 presents the formation error trajectories $y_i - y_r - \xi_i$, demonstrating rapid convergence to the desired configuration with minimal steady-state error. This performance confirms the controller's robustness in handling unmodeled dynamics and external disturbances.

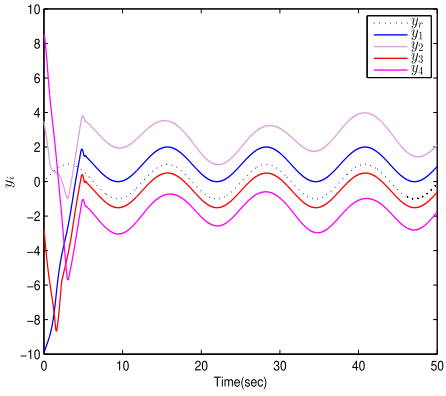

Figure 3. Outputs of followers y_i and reference signal y_r.

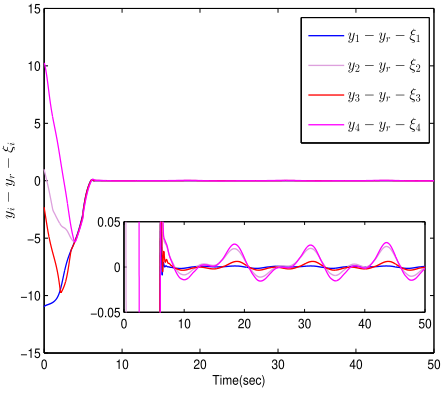

Figure 4. Formation tracking errors $y_i - y_r - \xi_i$.

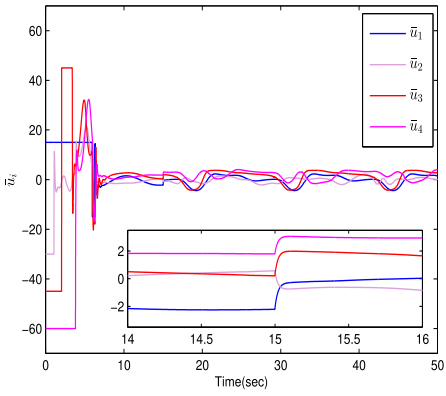

Figure 5. Actuator outputs $\bar{u}_i$.

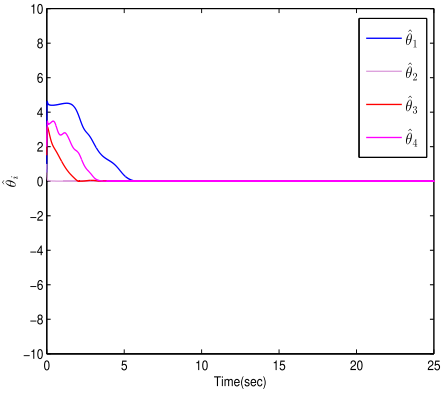

Figure 6. Adaptive parameters $\hat{\theta}_i$.

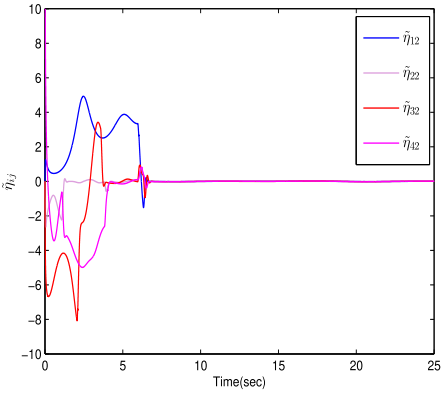

Figure 7. Filtering errors $\tilde{\eta}_{i,j}$.

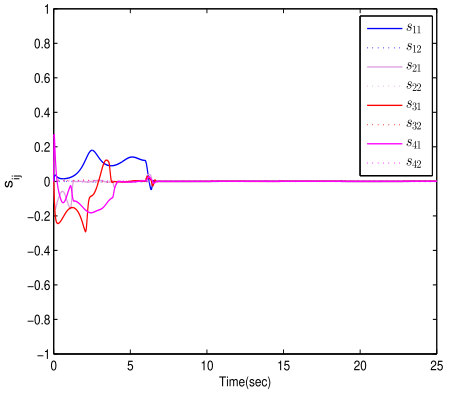

Figure 8. Compensation signals $s_{i,j}$.

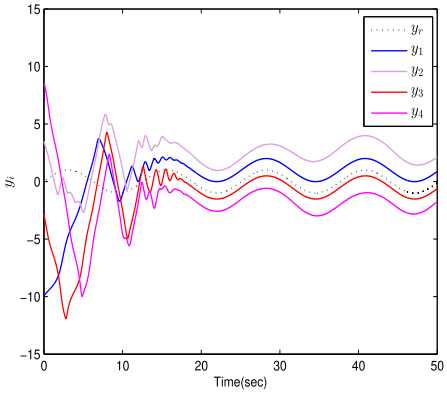

Figure 9. Outputs of followers y_i and reference signal y_r under finite-time control method.

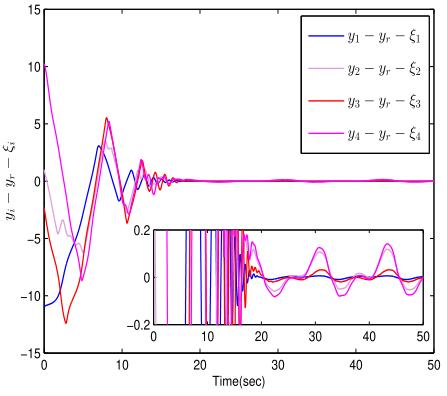

Figure 10. Formation tracking errors $y_i - y_r - \xi_i$ under finite-time control method.

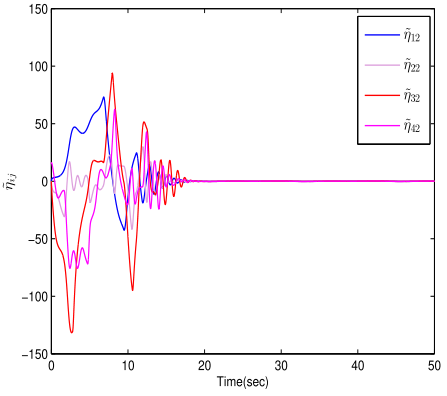

Figure 11. Filtering errors $\tilde{\eta}_{i,j}$ under finite-time control method.

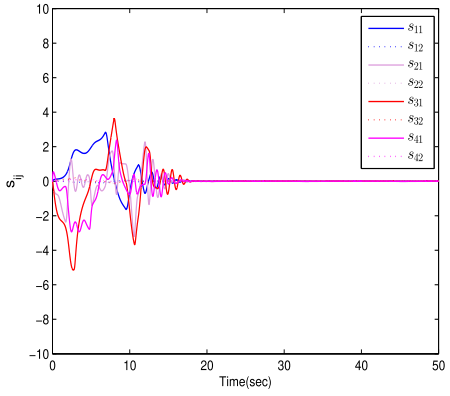

Figure 12. Compensation signals $s_{i,j}$ under finite-time control method.

The actuator outputs $\bar{u}_i$ shown in Fig. 5 indicate maintained formation integrity despite the introduction of nonaffine actuator faults at $t = 15$s. This observation validates the algorithm's effective management of input saturation nonlinearities and its strong fault tolerance. Adaptive parameter estimates $\hat{\theta}_i$ in Fig. 6 converge stably. Figures 7 and 8 present the filter errors $\tilde{\eta}_{i,j}$ and compensation signals $s_{i,j}$, respectively, providing quantitative verification of the theoretical findings in Lemmas 9 and 10. Collectively, these results establish the proposed PFTF scheme's effectiveness for multiship formation control, characterized by rapid convergence, high precision, and excellent disturbance rejection.

To demonstrate the superiority of the proposed PFTF control method, comparative verification is conducted against a finite-time control strategy under the same formation task. Paper [3] investigates finite-time cooperative control for nonlinear MASs subject to nonaffine faults. Employing the method from [3] with identical design parameters yielded the results shown in Figs. 9–12. While the finite-time approach achieves the

formation objectives, its performance is demonstrably inferior to the fixed-time scheme: Fig. 9 reveals a prolonged formation achievement time relative to Fig. 4, while Fig. 10 exhibits both slower convergence and degraded steady-state accuracy in the formation errors. Furthermore, Figs. 11 and 12 display the filter errors $\tilde{\eta}_{i,j}$ and compensation signals $s_{i,j}$ with significantly extended convergence periods and substantially larger overshoots compared to Figs. 7 and 8, suggesting potential implementation challenges in real-world applications. This comparative analysis validates that the proposed fixed-time control scheme successfully achieves PFTF for MASs and outperforms the finite-time method in convergence speed, steady-state precision, and robustness.

5 Conclusions

This paper investigates a PFTF control problem for heterogeneous MASs subject to coupled input nonlinearities and actuator faults. A distributed PFTF control scheme is developed by integrating command-filtered backstepping with NNs approximation techniques. The proposed strategy incorporates enhanced command filters, an error compensation mechanism, and both virtual and actual controllers paired with parameter adaptation laws. Notably, the protocol enables MASs to achieve fixed-time formation tracking, while confining formation errors to a small residual set. Simulation studies validate the efficacy of the control scheme. Future work will address prescribed performance constraints, collision avoidance, and extended operational scenarios.

Author contributions. All authors (J.J., J.L., C.H., and R.Z.) have contributed as follows: methodology, J.J. and J.L.; formal analysis, J.J. and J.L.; validation, J.L. and C.H.; writing – original draft preparation, J.J. and R.Z; writing – review & editing, J.L. C.H., and R.Z. All authors have read and approved the published version of the manuscript.

Conflicts of interest. The authors declare no conflicts of interest.

References

1. L. Cao, Z. Cheng, Y. Liu, H. Li, Event-based adaptive NN fixed-time cooperative formation for multiagent systems, *IEEE Trans. Neural Networks Learn. Syst.*, **35**(5):6467–6477, 2024, https://doi.org/10.1109/TNNLS.2022.3210269.
2. L. Cao, D. Yao, H. Li, W. Meng, R. Lu, Fuzzy-based dynamic event triggering formation control for nonstrict-feedback nonlinear MASs, *Fuzzy Sets Syst.*, **452**:1–22, 2023, https://doi.org/10.1016/j.fss.2022.03.005.
3. S. Cheng, B. Xin, Q. Wang, J. Chen, F. Deng, Finite-time neuroadaptive cooperative control for nonlinear multiagent systems under nonaffine faults and partially unknown control directions, *IEEE Trans. Cybern.*, **54**(12):7576–7589, 2024, https://doi.org/10.1109/TCYB.2024.3462832.
4. Z. Cuan, D.W. Ding, Fixed-time adaptive fuzzy tracking control for uncertain nonlinear cyber-physical systems against malicious attacks, *IEEE Trans. Network Sci. Eng.*, **11**(1):128–139, 2024, https://doi.org/10.1109/TNSE.2023.3292843.

5. Y. Deng, W. Zhu, Event-triggered leader-following formation control of general linear multi-agent systems with distributed infinite input time delays, *Nonlinear Anal. Model. Control*, **28**(4):760–779, 2023, https://doi.org/10.15388/namc.2023.28.32277.

6. G. Dong, H. Li, H. Ma, R. Lu, Finite-time consensus tracking neural network FTC of multi-agent systems, *IEEE Trans. Neural Networks Learn. Syst.*, **32**(2):653–662, 2021, https://doi.org/10.1109/TNNLS.2020.2978898.

7. H.Q. Hou, Y.J. Liu, J. Lan, L. Liu, Adaptive fuzzy fixed time time-varying formation control for heterogeneous multiagent systems with full state constraints, *IEEE Trans. Fuzzy Syst.*, **31**(4):1152–1162, 2023, https://doi.org/10.1109/TFUZZ.2022.3195609.

8. Q. Hou, J. Dong, Dynamic event-triggered fixed-time tracking control for state-constrained nonlinear systems with dead zone based on fast fixed-time filters, *IEEE Trans. Syst. Man Cybern.*, **54**(1):634–643, 2024, https://doi.org/10.1109/TSMC.2023.3317406.

9. J. Jiao, J. Li, Distributed fixed-time output consensus for disturbed second-order multiagent systems with dead-zone input, *Int. J. Syst. Sci.*, **55**(15):3166–3184, 2024, https://doi.org/10.1080/00207721.2024.2367075.

10. A. Kanchanaharuthai, E. Mujjalinvimut, Fixed-time command-filtered backstepping control design for hydraulic turbine regulating systems, *Renewable Energy*, **184**:1091–1103, 2022, https://doi.org/10.1016/j.renene.2021.12.004.

11. Q. Li, J. Wei, Q. Gou, Z. Niu, Distributed adaptive fixed-time formation control for second-order multi-agent systems with collision avoidance, *Inf. Sci.*, **564**:27–44, 2021, https://doi.org/10.1016/j.ins.2021.02.029.

12. X. Li, Z. Yu, D. Huang, H. Jiang, Finite-time and fixed-time sliding mode control for second-order nonlinear multiagent systems with external disturbances, *Nonlinear Anal. Model. Control*, **27**(6):1091–1109, 2022, https://doi.org/10.15388/namc.2022.27.29471.

13. Y. Li, F. Qu, S. Tong, Observer-based fuzzy adaptive finite-time containment control of nonlinear multiagent systems with input delay, *IEEE Trans. Cybern.*, **51**(1):126–137, 2021, https://doi.org/10.1109/TCYB.2020.2970454.

14. J. Ma, H. Wang, J. Qiao, Adaptive neural fixed-time tracking control for high-order nonlinear systems, *IEEE Trans. Neural Networks Learn. Syst.*, **35**(1):708–717, 2024, https://doi.org/10.1109/TNNLS.2022.3176625.

15. A. Polyakov, Nonlinear feedback design for fixed-time stabilization of linear control systems, *IEEE Trans. Autom. Control*, **57**(8):2106–2110, 2012, https://doi.org/10.1109/TAC.2011.2179869.

16. M.M. Polycarpou, Stable adaptive neural control scheme for nonlinear systems, *IEEE Trans. Autom. Control*, **41**(3):447–451, 1996, https://doi.org/10.1109/9.486648.

17. Y. Salmanpour, M.M. Arefi, J. Cao, Event-triggered adaptive preassigned finite-time consensus control for multiagent systems with nonlinear faults, *IEEE Trans. Cybern.*, **54**(12):7392–7403, 2024, https://doi.org/10.1109/TCYB.2024.3443352.

18. P. Shi, B. Yan, A survey on intelligent control for multiagent systems, *IEEE Trans. Syst. Man Cybern.*, **51**(1):161–175, 2021, https://doi.org/10.1109/TSMC.2020.3042823.

19. J. Sui, C. Liu, B. Niu, X. Zhao, D. Wang, B. Yan, Prescribed performance adaptive containment control for full-state constrained nonlinear multiagent systems: A disturbance observer-based design strategy, *IEEE Trans. Autom. Sci. Eng.*, **22**:179–190, 2025, https://doi.org/10.1109/TASE.2023.3348978.

20. S. Sui, C.L.P. Chen, S. Tong, A novel full errors fixed-time control for constraint nonlinear systems, *IEEE Trans. Autom. Control*, **68**(4):2568–2575, 2023, https://doi.org/10.1109/TAC.2022.3200962.

21. K. Sun, L. Liu, J. Qiu, G. Feng, Fuzzy adaptive finite-time fault-tolerant control for strict-feedback nonlinear systems, *IEEE Trans. Fuzzy Syst.*, **29**(4):786–796, 2021, https://doi.org/10.1109/TFUZZ.2020.2965890.

22. S. Tong, K. Sun, S. Sui, Observer-based adaptive fuzzy decentralized optimal control design for strict-feedback nonlinear large-scale systems, *IEEE Trans. Fuzzy Syst.*, **26**(2):569–584, 2018, https://doi.org/10.1109/TFUZZ.2017.2686373.

23. J. Wang, Y. Li, Y. Wu, Z. Liu, K. Chen, C.L.P. Chen, Fixed-time formation control for uncertain nonlinear multi-agent systems with time-varying actuator failures, *IEEE Trans. Fuzzy Syst.*, **32**(4):1965–1977, 2024, https://doi.org/10.1109/TFUZZ.2023.3342282.

24. K. Wang, X. Liu, Y. Jing, Adaptive finite-time command filtered controller design for nonlinear systems with output constraints and input nonlinearities, *IEEE Trans. Neural Networks Learn. Syst.*, **33**(11):6893–6904, 2022, https://doi.org/10.1109/TNNLS.2021.3083800.

25. P. Wang, C. Yu, M. Lv, Optimized formation control of nonlinear systems with full-state constraints using adaptive fixed-time techniques, *IEEE Trans. Autom. Sci. Eng.*, **22**:3331–3344, 2025, https://doi.org/10.1109/TASE.2024.3392936.

26. Q. Wang, Y. Hua, X. Dong, P. Shu, J. Lü, Z. Ren, Finite-time time-varying formation tracking for heterogeneous nonlinear multiagent systems using adaptive output regulation, *IEEE Trans. Cybern.*, **54**(4):2460–2471, 2024, https://doi.org/10.1109/TCYB.2023.3245139.

27. X. Wang, D. Ye, Finite-time output-feedback formation control for high-order nonlinear multiagent systems with obstacle avoidance, *IEEE Trans. Autom. Sci. Eng.*, **21**(2):1878–1888, 2024, https://doi.org/10.1109/TASE.2023.3244536.

28. W. Wu, S. Tong, Collision-free adaptive fuzzy formation control for stochastic nonlinear multiagent systems, *IEEE Trans. Syst. Man Cybern.*, **53**(9):5454–5465, 2023, https://doi.org/10.1109/TSMC.2023.3268663.

29. H. Yang, D. Ye, Adaptive fixed-time bipartite tracking consensus control for unknown nonlinear multi-agent systems: An information classification mechanism, *Inf. Sci.*, **459**:238–254, 2018, https://doi.org/10.1016/j.ins.2018.04.016.

30. W. Yang, Z. Shi, Y. Zhong, Distributed robust adaptive formation control of multi-agent systems with heterogeneous uncertainties and directed graphs, *Automatica*, **157**:111275, 2023, https://doi.org/10.1016/j.automatica.2023.111275.

31. G. Yuan, Z. Zhang, C. Qin, S.S. Ge, Adaptive control for nonlinear time-varying systems with unknown control coefficients and external disturbances, *IEEE Trans. Syst. Man Cybern.*, **54**(1):119–130, 2024, https://doi.org/10.1109/TSMC.2023.3304451.

32. X. Zheng, H. Ma, D. Yao, H. Li, Neural-based predefined-time distributed optimization of high-order nonlinear multiagent systems, *IEEE Trans. Artif. Intell.*, **5**(6):3174–3183, 2024, https://doi.org/10.1109/TAI.2023.3343684.

33. X. Zheng, X. Yu, X. Yang, J.J. Rodriguez-Andina, Practical finite-time command-filtered adaptive backstepping with its applications to quadrotor hovers, *IEEE Trans. Cybern.*, **54**(5): 3017–3029, 2024, https://doi.org/10.1109/TCYB.2023.3323664.

34. X. Zhou, C. Huang, P. Li, Z. Ma, J. Cao, Leader-following identical consensus for markov jump nonlinear multi-agent systems subjected to attacks with impulse, *Nonlinear Anal. Model. Control*, **28**(5):995–1019, 2023, https://doi.org/10.15388/namc.2023.28.33003.

35. Z. Zuo, R. Ke, Q.L. Han, Fully distributed adaptive practical fixed-time consensus protocols for multi-agent systems, *Automatica*, **157**:111248, 2023, https://doi.org/10.1016/j.automatica.2023.111248.